MASTER DEGREE OF MINING ENGINEERING

MASTER DEGREE THESIS

# Performance analysis of cutting tools from ILCM tests through computer-aided modeling methods

Tutor:
Ing. Prof. Dr. Marilena Cardu

Candidate :
Kursat Kilic

Academic Year 2019/2020

October, 2020

# MASTER THESIS OUTLINE

## Introduction ;

**Chapter – 1 ;**

(History of tunnelling / Historical Development Of Tunnelling)

**Chapter – 2 ;**

Types Of TBM ( General Information About TBM Tunnelling )

- Hard rock (Open TBM ; Single Shield; Double Shield)
- Soft rock

TBM Performance In Hard Rock

Selection Cretaria Of TBM

**Chapter - 3 ;**

Rock Cutting Tools And Theories

Cutter Tools Mechanism

Mechanism Of Chip Formation

Performance Prediction Of Cutter Tools Methods (Theoratical And Analytic)

**Chapter – 4 ;**

Computer Aided Modelling Methods For Cutter Tool Performance Prediction

**Chapter – 5 ;**

Linear Cutting Machine

- Properties
- Performance Scaling

Intermediate Linear Cutting Machine

- Properites
- Scaling

**Chapter - 6 ;**

Computer Aided Modelling Test Results And Interpretation

- Data Analysis (Data of Luserna Stone, Prali Marble, Diorite)

**7. Conclusion**

**8. References**

*The thesis is dedicated to my parents and my friends*

*For their endless love, support and encouragement*

## Acknowledgement

Foremost, I would like to express my sincere gratitude to my advisor Prof Dr Marilena Cardu, for the continuous support of my master study and thesis, for her patience, motivation, enthusiasm, and immense knowledge. Her guidance helped me in all the time of writing this thesis. I could not have imagined having a better advisor and mentor for my MSc study.

## THESIS CONTENT

# FIGURE INDEX

## Table List

# INTRODUCTION

This study is realized with the aim to evaluate the performance analysis of TBM's (Tunnel Boring Machine) disc cutters through computer-aided modeling methods, such as IBM SPSS Statistics 25.

According to real projects and to some research activities, it has been justified that , due to its high safety, good productivity and less environmental impacts, TBM tunneling is the most suitable technique for civil engineering purposes in urban areas.

As quoted by (Barla, 2014), the TBMs are categorized as the Gripper TBM, Single Shield TBM and Double Shield TBM. The TBMs uses the cutter head from 1 m to 19 m.

According to (Bilgin, 2013), the EPB/TBM is operated in soft ground, and the excavated material is used for support.

For the performance analysis of the TBM in hard rock, several models are used in literature. For instance, the QTBM model (Barton, 1999; Barton, 2000) utilizes the rock mass classification system. The NTNU model (Bruland et al., 1995) is a kind of empirical model, and it uses rock mass properties with machine parameters for performance analysis. Another approach is presented by (Roxborough and Phillips, 1975); the disc cutters are affected by their geometry and rock strength.

The CSM model (Ozdemir, 1997), is based on the V - profile type disc cutter, and it has been modified with industrial experience.

As quoted by (Bilgin, 2013), in boulder rock conditions, the chisel and disc cutter are used together during advancement.

As quoted by (Xu et al., 2019), some computer-aided modelling has been applied to TBM performance analysis. For instance, KNN (k-Nearest Neighbor), SVM (support vector machine), artificial neural network (ANN), CART ( classification and regression trees), CHAID (Chi-Squared Automatic Interaction Detection), Non - Linear Multiple Regression Analysis, Neuro-Fuzzy Modelling and SPSS Analysis.

Furthermore, according to (Pan et al., 2019; Balci, 2009), the LCM (Linear Cutting Machine) is the more reliable and correct method for performance analysis because it provides practical rock cutting force and efficient cutter spacing, thrust and torque.

On the other hand, the TBM disc cutter performance analysis has been done by using ILCM's outputs data (Intermediate Linear Cutting Machine). The ILCM has some advantages than the LCM in terms of handling and positioning of the rock samples.

For this dissertation work, the data which have been acquired from Italian stones such as the Vico Diorite, Luserna stone and Prali marble used.

To summary, the thesis will provide elaborative results in terms of ILCM disc cutter performance analysis by using IBM SPSS linear regression models among the rock and machine interaction parameters such as specific energy, normal force, rolling force, s/p, cutting coefficient.

All information, as mentioned above, is explained deeply in the following pages.

# 1 CHAPTER – 1 LITERATURE REVIEW;

## 1.1 History Of Tunnelling

Tunnelling was used for water, warfare and to enlarge the caves by ancient people about 3000 B.C. There were different examples of ancient tunnelling in historical researches such as in Babylonia, underground space construction which was a kind of tunnel used for irrigation and pedestrian way to accessed from Euphrates river to royal palace. In addition to these, during the middle age, tunnelling was performed to extract minerals and to applied military engineering. In the 17th century, tunnels were constructed uniquely for linking ocean to sea for transportation activities, such as Canal du Midi (known as Languedoc) tunnel in France (1666 – 81), which was built by Pierre Riquet from Atlantic to the Mediterranean. Furthermore, in 1830, railroads were introduced, and more appropriate means for transportation were implemented so that demand for tunnelling was increased dramatically. After that development, in 1830, a 3.5-mile tunnel was built as a railroad from Manchester to Sheffield (1839 – 45) (Kenneth S. Lane, 1999 (URL-1), ; Wiley Book Ch (URL-2)).

Simultaneously, the outstanding tunnel was commenced in the Alps, which is known as Mount Cenis Tunnel (Frejus). The hydraulic ram air compressors and integrated drilling machine were used to build the tunnel in the construction stage. In 1855, one of the most important developments in history occurred thanks to Hoosac tunnel, thanks to the first use of the electric initiation of explosives and to power drills that were performed during operation. That was the breaking point of tunnelling technology in terms of the compressed air industry. (Kenneth S. Lane, 1999 (URL-1) ; Wiley Book Ch (URL-2)). The history of tunnelling hasn’t had only development, but also hazardous accidents and complicated engineering. One of the first examples of an accident in the tunnel industry was Lötschburg in 1908. During the construction of a part of a tunnel under the Kander River valley, a high amount of water flew into the tunnel with sand, rock, gravel and other material, consequently, 25 employees were buried under the debris.

In the modern world, the tunnelling industry has developed breakthrough technologies and machines to avoid disasters as mentioned above and to gain time for long-distance tunnelling. For instance, mechanized (machined) tunnelling method such as TBM (Tunnel Boring Machine) has been improved to increase safety and the performance of excavation in tunnelling operations. The first example of TBM (Figure.1.1) was used in the Channel Tunnel by the Beaumont machine. However, the construction was not accomplished because of several hard conditions, unexpected tunnel instability and insufficient technological facilities.

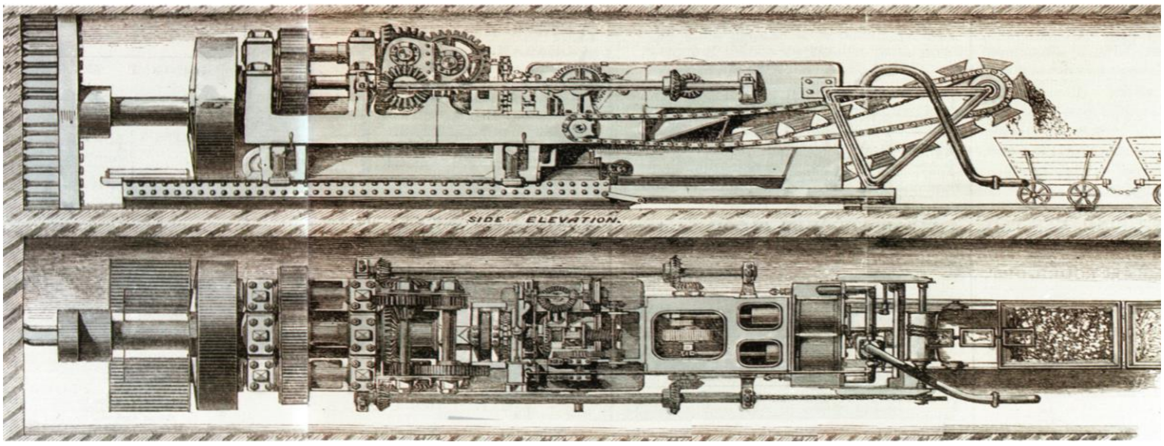


Figure 1-1 : A contemporary plan of a tunnel boring machine from the 1880s on an idea by Colonel Frederick Beaumont and Thomas English (Wikipedia : https://commons.wikimedia.org/wiki/File:Beaumont-tunnelbohrmaschine.png

After that, in 1851, the American engineer Charles Wilson manufactured and improved a TBM. It could be said that he approached the first example of mechanized-tunnelling, using disc cutters that were mounted on the TBM face and a given thrust force that was adjusted to sustain the proper excavation. Afterwards, until the 1950s, TBM industry did not experience innovation, until James S. Robbins invented the first open TBM for Hummer sewer tunnel seen Figure in 1.2 so that the advancement became the milestone of mechanization in the tunnel industry.

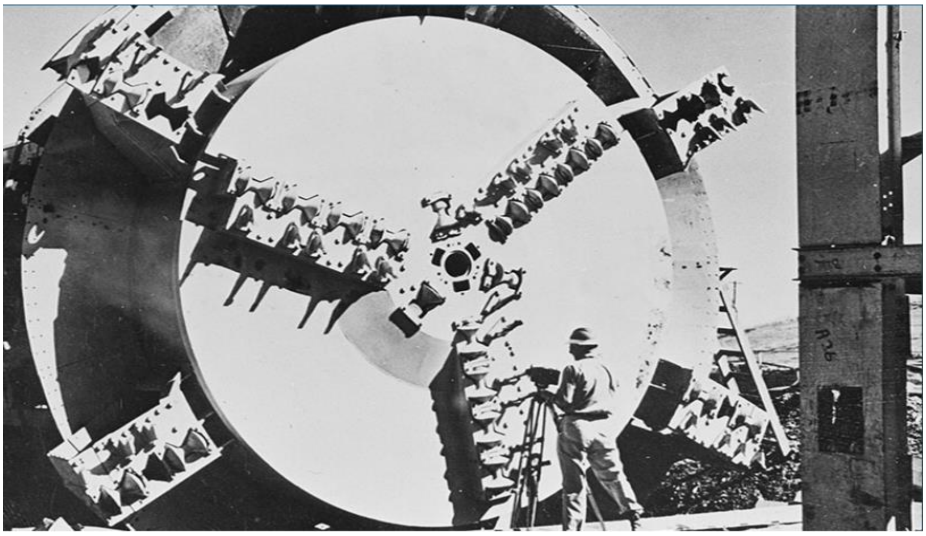

Figure 1-2 : James S. Robbins Open TBM, 1953. 8 meters diameter (Robbins website - https://www.therobbinscompany.com/)

# 2 CHAPTER – 2

## 2.1 Tunnel Boring Machines

According to (Barla, 2014) TBMs are classified as Gripper TBM, Single Shield TBM and Double Shield TBM. The TBM excavation is performed in by using vertical cutter heads which are from 1 meter to about 19 meters (the largest one) in various geological conditions. Meanwhile, the working principle of TBM is the rotating the cutterhead apply pressure towards the disc and the disc roll around the tracks to the face, and then the disc pressure exceeds compression strength of the rock, so the discs penetrate the face (Barla, 2014), (Maidl, 2008). Therefore, the cutting edge of the disc goes into the rock until to get the balance between advance force and hardness of the rock mass so that it reaches the net penetration and creates a long piece of rock (chips) breaking off (Barla, 2014). The operators, monitor and control thrust on the cutter head, during the advancement of the TBM into the rock mass, in case of the too-high magnitude of thrust and too slow rotation. Because of these low parameters lead to failing the TBM and also the discs are worn out. Nevertheless, a moderate amount of thrust and too fast rotation do not provide to forward the machine. Hence, cutter head rotates around the same position, and it leads to collapse the roof of the tunnel that situation is dangerous, especially undersea operations (Kuesel, 2012).

### 2.1.1 Open Type (Open Gripper) TBMs

Hard rock TBM types are called Open-type TBMs or Gripper TBM. The TBMs are operated in hard rock and low discontinuities (Bilgin, 2013). The TBMs are most affordable in terms of operating cost when the rock does not require permanent support such as rock anchors, steel archers or shotcrete (Maidl, 2008). Besides, working principles of the Gripper TBMs (Chapman et al., 2010) are defined as to implement the thrust (normal) force to the cutterhead. The machine is attached encounter the tunnel sidewall with hydraulically driven attached shoes, generally called grippers and then the hydraulic system operates cutter head towards to face approximately 0.7 m to 1.2 m. Afterwards, the cutter head is stopped to forward the tail of the machine, auxiliary supports are supplied behind the cutter head, and hydraulic jack advances the cutter head towards to face and the tail of the machine is pulled forward. On the authority of Maild (2008), hard rock TBMs consist of the boring section, cutterhead, clamping part, muck removal section and the support section (Barla, 2014), (Chapman, 2017). Furthermore, according to (Bilgin et al., 2013), the relationship between diameter and thrust for open-type TBMs in terms of various UCS, seen in Figure 2.1. As an example of open type, TBM is given in Figure.2.2.

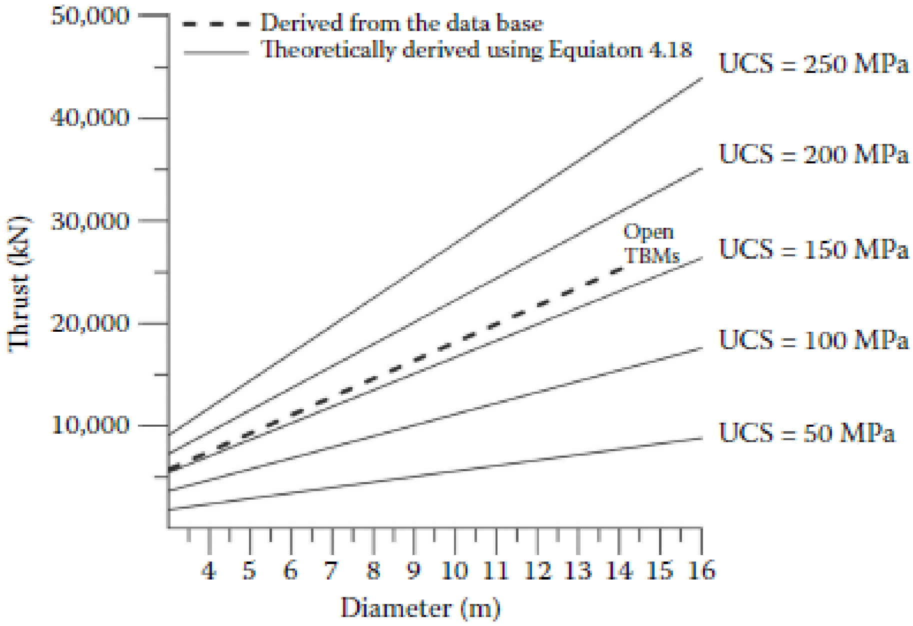


Figure 2-1 : Relationship between diameter and thrust force for open type TBM for different rock compressive strengths (Bilgin, 2013)

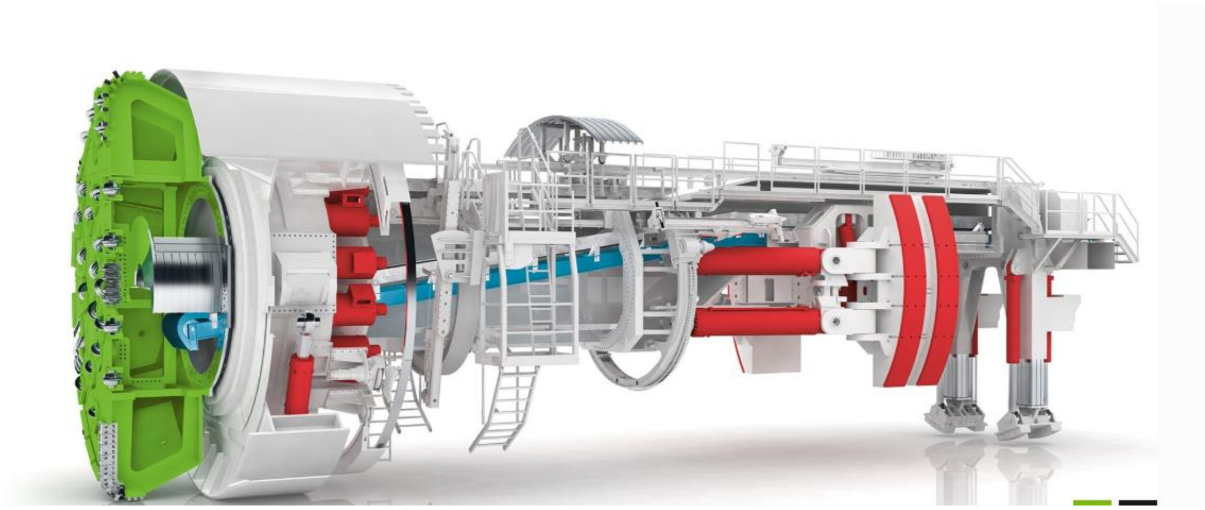

Figure 2-2 : Gripper TBM Φ 2–12.5m (Herrenknecht – https://www.herrenknecht.com/de/)

### 2.1.2 Single Shield TBMs

Singl-shield TBMs (Figure.2.3) operate in rock mass which is rarely weak and discontinuous. The cutter head and mucking system are not different from the open TBM, but the shield protects the operator, machine’s personnel and other parts of the equipment. The function of shield system is similar to the Gripper (open) type TBMs but the advancing movement (thrust) is supplied by precast segments and structure of the shield begin from behind the cutter head to the whole machine. The construction stage of the tunnel is sustained under the protection shield, and also reinforcement concrete system is generally used as a support during the tunnel construction. Moreover, the working cycle consists of three steps, i.e., advancement for a distance equivalent to the stroke of the thrust jack, combined of concrete segments and pullback of the jacks and as a final stage, new excavation rub (Bilgin, 2013; Chapman,2017; Guglielmetti, 2008). One of the most important advantages of the single shield TBMs is the possibility to be converted as closed mode, in case of the high amount of groundwater immersion during construction.

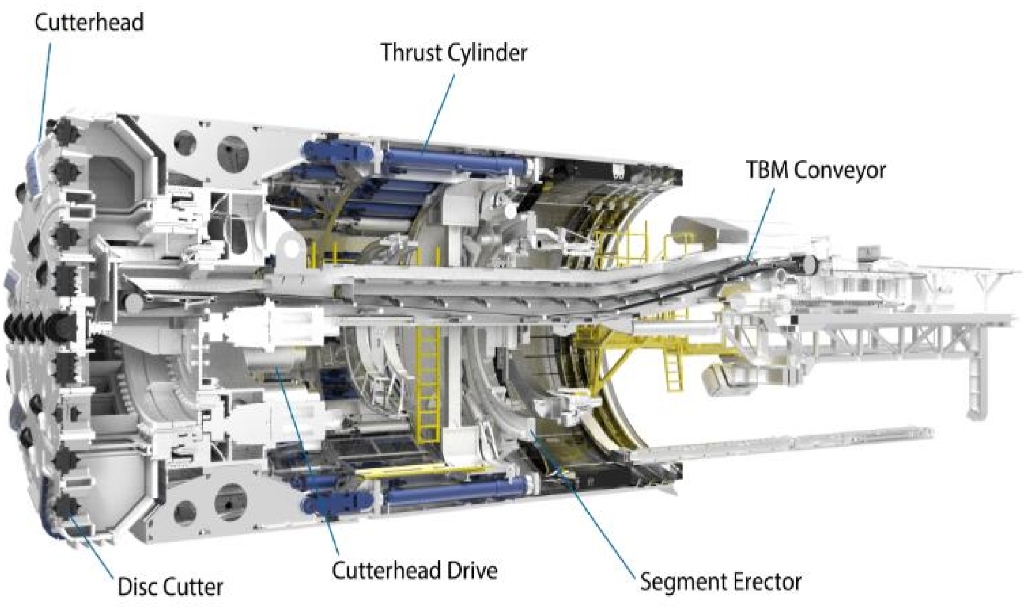


Figure 2-3 : Single – Shield TBM Robbins Φ 1.6 to 15 m (Robbins website - https://www.therobbinscompany.com/)

### 2.1.3 Double – Shield TBMs

The double shield TBM (Figure 2.4) is also known as telescopic type TBM because it has a telescopic system (Figure.2.5). This TBM type is implemented in fractured rock masses and low stand-up time excavation profile. Moreover, advancement principle of the double shield TBM is the TBM movement depends on the gripper shoes, which are anchoring itself to the sidewall of the tunnel while excavation and support segment installation operates at the same time (Bilgin, 2013; Chapman, 2017). The double shield TBM is performed both in double shield mode, to obtain high advance rate, and single shield if the grippers can not be applied during tunnel construction. The TBM has some advantages such as it can work under critical zones, the advance rate is faster, and by means of telescopic movement, the cutter head is prevented from blockage due to collapsing material (Grandoril et al., 2018).

The main component of double shield TBM is a cutterhead, protective shield and single or double thrust system, respectively (V. Guglielmetti, 2008)

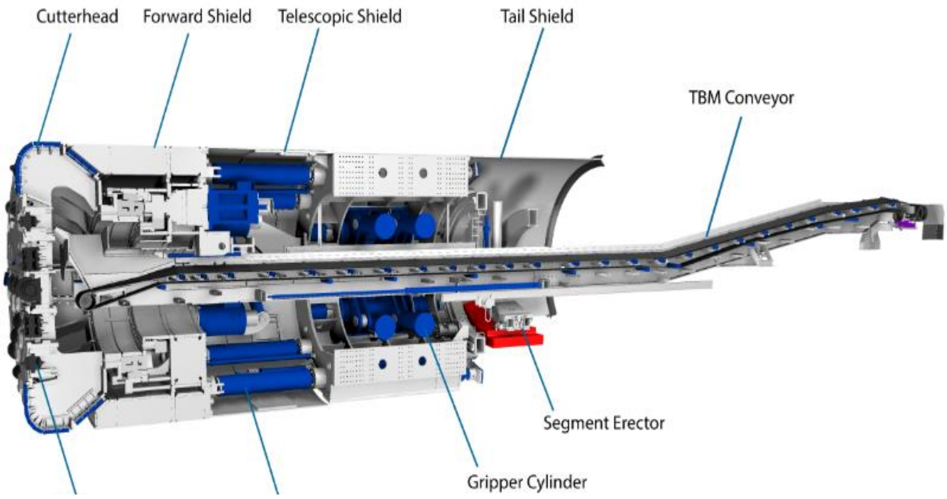


Figure 2-4 : Double Shield TBM Robbins (Robbins website - https://www.therobbinscompany.com/)

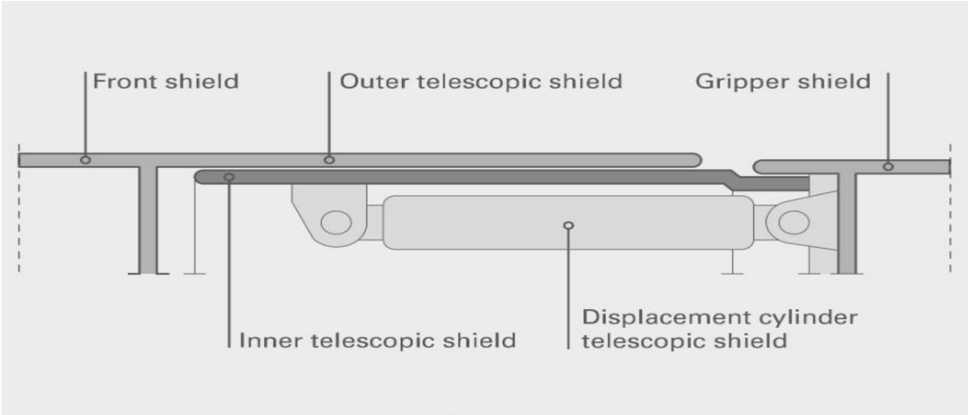


Figure 2-5 : Double Shield Telescopic System – (Herrenknecht website https://www.herrenknecht.com/de/)

### 2.1.4 Soft Ground Tunnelling Machines

#### *2.1.4.1 Slurry Tunnelling Machines(Mixshield)*

The STMs include two types of machines which are fluid type and air bubble type. According to (D.Chapman et al., 2017), the slurry tunnelling machine in Figure.2.6 applies a compressed fluid to stabilize the face while advancing in the ground. The air bubble type machine provides a considerable amount of compressed air into the plenum (is a kind of chamber) in the roof behind the cutter head so that a constant pressure provides at the face. Whatsmore, during the excavation process, the STMs mix the excavated materials for transportation with the pumping system. Besides, the STMs include a sort of crusher in Figure 2.7, which is mounted behind a cutter head to break large size of rock pieces before transportation. Afterwards, the pressurized fluid is pumped outside the operation site to separates particles from the liquid by using cyclones and screenings like in the mineral processing plants. If the excavated material has just a fine (cohesive) properties, water is used for transportation. In contrast, bentonite applies if the excavated material consists of sand and gravel, to get pumping correctly (D. Chapman, 2017).

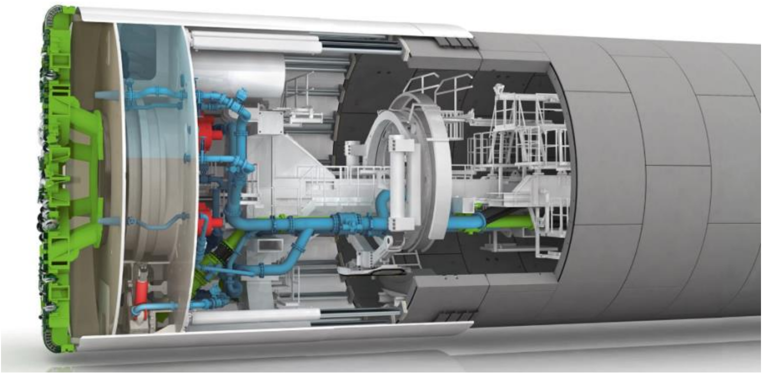

Figure 2-6 : Slurry Tunnelling Machine Herrenknecht (Mixshield) (Herrenknecht website - https://www.herrenknecht.com/de)

Figure 2-7: Slurry Type Crusher Unit Herrenknecht (Herrenknecht website - https://www.herrenknecht.com/de)

This mix shield TBM has been designed as a single chamber of the conventional slurry shield by Herrenknecht, Wayss & Freytag (Maidl et al.,2013). The pressure at the tunnel face is managed more effectively rather than a traditional slurry type, and the mix shield TBM decreases the subsidence risk while excavating under cities. The TBM is widely performed in a non-cohesive soil formation, which needs liquid face support. The bentonite is used as support and conveyor for excavated materials, and its density impacts on the function of the mix shield. Furthermore, to acquire an efficient operation of mix shield, more extensive space and comprehensive separation technology are required to reduce high bentonite density. (Herrenknecht and Rehm, 2003) .

#### *2.1.4.2 EPB ( Earth Pressure Balance ) Tunnelling Machine*

EPB tunnelling machine that is demonstrated in Figure.2.8, operates in soft ground conditions (Bilgin, 2013) and, during the construction stage of the tunnel, it uses excavated materials as a support for tunnel lining. The excavated material moves into the plenum within a fluid or plasticised state after mixing with soil chemical conditioners. Apart from the other conveying devices, the EPB uses a screw conveyor system to transport the excavated material: it fills into the cutter head opening pressure chamber where the soil conditioning process occurs. Hydraulic cylinders provide thrust while the excavated materials are transported from the pressure chamber to outside of the machine by using screw conveyor (Bilgin, 2013) and the face support is managed by the screw rotation speed (Guglielmetti, 2008 ). Furthermore, in excavation and conditioner process, some additives (chemicals) are used, such as high-density mud or foams. Utilising that additives, the machine is capable of excavating sandy-gravely or gravely ground (Guglielmetti, 2008). Whatsmore, this EPB has three types such as closed mode EPB, compressed air and open mode as well. It depends upon the grain size distribution in Figure.2.9, EPB – TBM is prefered in silt and clay formation, whereas the slurry EPB is operated in sand and gravel formations (Chapman,2010).

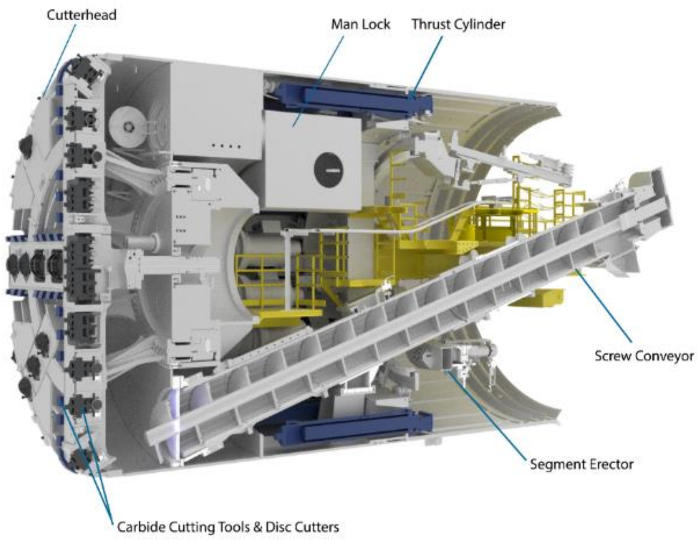


Figure 2-8: EPB TBM Robbins (Robbins website - https://www.therobbinscompany.com/)

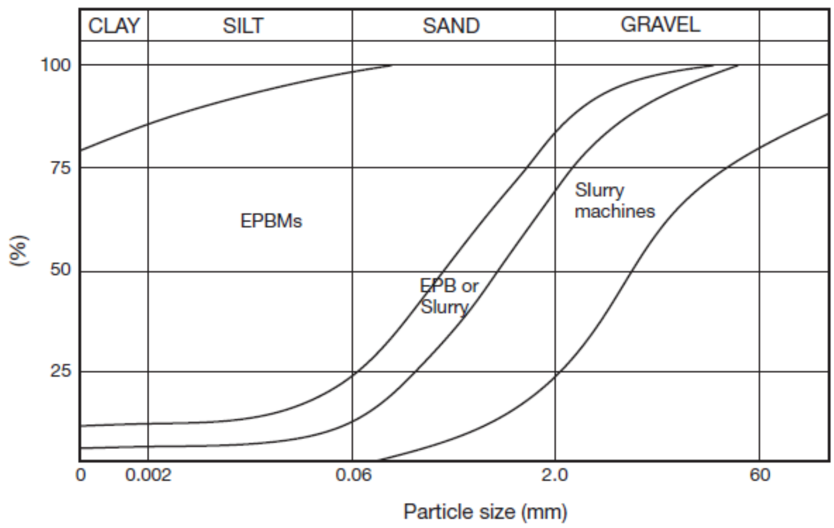


Figure 2-9 : Grain Size Distribution Choice Of EPBs and Slurry TBM ( D. Chapman,2010)

## 2.2 TBM Performance In Hard Rock

Determining the most appropriate TBM is a vital issue in tunnelling projects so that one of the most critical decision is the performance of TBM in those projects. For analysis of TBM performance, laboratory test, site observations and computer-aided modelling methods are applied (Afrasiabi, 2019).

According to Rostami (2002), geometrical features of TBM and the rock mass properties impact the disc cutters while cutting the rock. Besides, the size and shape of the rock, are related to penetration and spacing of the disc cutter tools. On the other hand, the chipping is a more effective excavation operation because producing chips through tensile fracturing is much more effective than the formation of fines in the crushed zone (Villeneuve, 2017). The formation of chips by the chipping process is therefore critical for achieving high penetration rates. Furthermore, different joints orientation, seen in Figure.2.10, and different spacing, shown in Figure.2.11, have considerable influence on required thrust and torque for TBM the chip size and cutting performance (Howarth, 1981;Bruland, 2000; Afrasiabi et al., 2019).

Another consideration of TBM performance had been provided by (Aeberli and Wanner, 1978), who stated that some discontinuities have a higher impact on TBM performance than others. For instance, discontinuities parallel to advance axis of TBM, the lowest positive effect on the TBM performance while the orientation of $60^o$ to advance axis has the highest influence (Aeberli and Wanner, 1978).

Other concern about TBM performance analysis has been presented by (Einstein et al.,1992) and Einsteing (2001). They are related to more data variables such as geological properties, machine operation, site parameters and management within the performance of the machine using histogram of several input data (Rostami, 2016).

According to Barton, (1999), Barton (2000), Q system is a kind of rock mass classification system in geomechanics field. Barton had added some new data to forecast TBM performance and application. Employing this new model which is called QTBM, a high number of input data has been applied such as RQD, joint conditions, intact rock strength, quartz content and TBM thrust force to estimate QTBM and as a consequence penetration rate and advance rate had been evaluated (Hassanpour, 2011).

One of the other TBM performance analysis approaches has been provided by NTNU (Norweigan Science And Technology University, Listrud 1988; NTH 1995; Bruland et al., 1995). Some empirical analysis and regression graphs have been performed to analyze TBM performance by using rock properties, drilling index and machine parameters. The parameters are shown in Table.1.

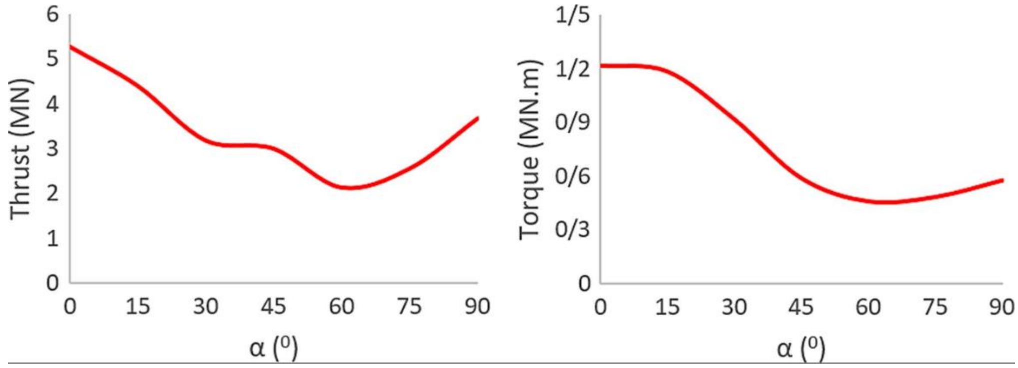


Figure 2-10: Required thrust (left side) and torque (right side) for different orientationa (Afrasiabi,2019)

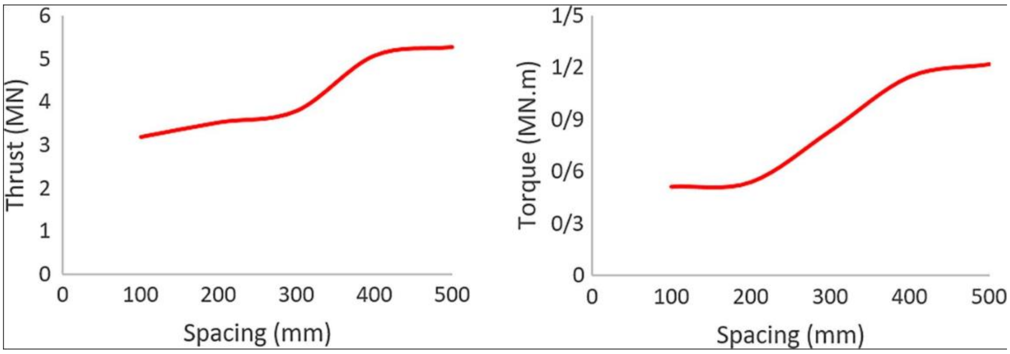


Figure 2-11:Thrust (left side) and torque (right side) required for different spacing (N. Afrasiabi,2019)

| Rock Mass Properties | Machine Parameters |
|---|---|
| • **Fracturing, Joints**<br>• **Drilling rate index (DRI)**<br>• **Abrasivity, CLI** | • Cutter Thrust<br>• Cutterhead RPM<br>• Cutter Spacing<br>• Installed Power |

Table 1:Parameters of NTNU Model

After that, the parameters were linked to UCS and abrasiveness. The fundamental testing begins with a set of applications:

- Brittleness test "$S_{20}$" is defined as percentage of material that passes the 11.2 mm mesh after the aggregate has been crushed by 20 impacts in the mortar
- Sievers' J index "$S_j$" is used to measure depth of penetration by using miniature drill bit, bit weight and number of rotation.

- Abrasion testing “AV”, is the average value of the measured weight loss in miligrams of 2 – 4 tungsten carbide test bits after 5 minutes. (Rostami et al., 1996).

The output of these test is used in proper charts such as drilling rate index (DRI), cutter life index (CLI), bit wear index (BWI) and correction factor with load capacity and machine diameter etc. to estimate base penetration. The penetration is then converted into net penetration rate.

Apart from the other performance analysis models, the CSM (Colorado School Mines) method has been widely used in industry. The CSM model is associated with cutter forces, overall thrust, torque and power supplied to the cutter head. Moreover, predicted values are compared with machine installation, appropriate thrust and power; the highest accomplishable penetration rate can be acquired (Rostami et al., 1996). As a result, TBM performance analysis is calculated by using these parameters in the CSM model.

All these models will be explained more in detail in chapter 3 in terms of dics cutter performance analysis.

### 2.3 TBM Selection Criteria

In order to determine the most convenient TBM type, some specific parameters are evaluated by producer/designer and industry. The following properties are considered and shown in Table.2 :

- Geology
- Site information
- Restrictions use of products
- Capital cost
- Orientation (Vertical and Horizontal)
- Experience and knowledge
- Train configuration (Lovat, 2006).

| | |
|---|---|
| **Geology** | • Type of soil, rock and ground condition<br>• Water content<br>• Mechanical properties of rock mass<br>• Grain size ditribution curve |
| **Tunnel Alignment** | • Vertical and horizontal curves<br>• Slope of the tunnel<br>• Ergonomics of operation<br>• Depth of tunnel<br>• Number of drifts and shafts |
| **Site Restrictions** | • Size of operation in a given site<br>• Location of operation can restrict installation activity<br>• Avaiable Equipment<br>• Restricted Access<br>• Shaft Dimension |
| **Additives (EPB TBM)** | • Water<br>• Foam<br>• Polymer<br>• Bentonite<br>• Agents |
| **Buyer Experience and Local Knowledge / Support** | • Experience level of contractor<br>• Local work force<br>• Local infrastructure for support<br>• Outside assistance and local companies for equipments |
| **Critical Structures** | • Monuments<br>• Old buildings<br>• Proximity to other underground structures |
| **Project Time Table** | • Refurbishing<br>• Already available equipment<br>• In case of SPB machine, surface processing plant size<br>• Rate of advancement |
| **Items for TBM Design** | • Machine Diameter<br>• Segment Handling<br>• Lenght of the machine<br>• Max segment width<br>• Size of muck train (EPB)<br>• Tranin Configuration |

Table 2: Selection Criteria Of TBM (Lovat, 2006)

# 3 CHAPTER – 3

## 3.1 Rock Cutting Tools And Theories

Concept of mechanical rock cutting should be understood by researchers, students and engineers in order to minimize large costs of trial – and – error. Besides, the capability of the excavation machine performance in hard rock is restricted by rock mass stiffness and the durability of cutting tools to high forces. The high forces lead to damage cutting tools and also damage the other parts of the machine by surpassing the machine's torque and thrust limit. (Bilgin, 2013). For this purpose, various rock – cutting performance analysis and then experimental studies will be given to better understand interaction of rock and cutter tools.

Wedge and chisel cutter tools are used in road headers, continuous miner and drum shearer. In contrast, the disc cutter is implemented in TBM to excavate from medium strength to harsh rock conditions (Bilgin, 2013). Many cutting theories have been developed for simple chisel cutter tools because the geometrical properties of those tools are simple and also can be adjusted by several parameters, e.g., ridge angle, bottom angle and wearing (Bilgin, 2013). The chisel cutters, which are a variety of drag type tools, cut the rock by using a dragging action. In most cases, chisel tools and disc cutter tools are employed in cutterhead of TBM (Figure.3.1), due to cutting boulders called cobbles and pebbles (Bilgin et al., 2012).


Figure 3-1:Dics and chisel cutters together (Bilgin, 2012)

### 3.1.1 Simple Chisel Cutters

Chisel cutter tools are considered by using dependent and independent parameters. The independent values are depth of cut, width of tool, rake angle, clearance angle and cutter spacing, respectively. In contrast, the dependent parameters are cutting force (FC), normal force (FN), breakout angle (Θ), yield (Q) and specific energy. Depending on chipping and brittleness of rocks, the force which is acting on the cutter tools is continuously arranged. The chisel cutter tools have a sort of peak to mean force ratio based on rock mass properties so generally between 1,5 and 3, but if the rock is brittle, the ratio is higher. Also, the ratio of cutting force and normal force is 2 for sharp tools. Furthermore, the recorded forces for chisel tools shown in Figure 3.2 (Bilgin, 2013).

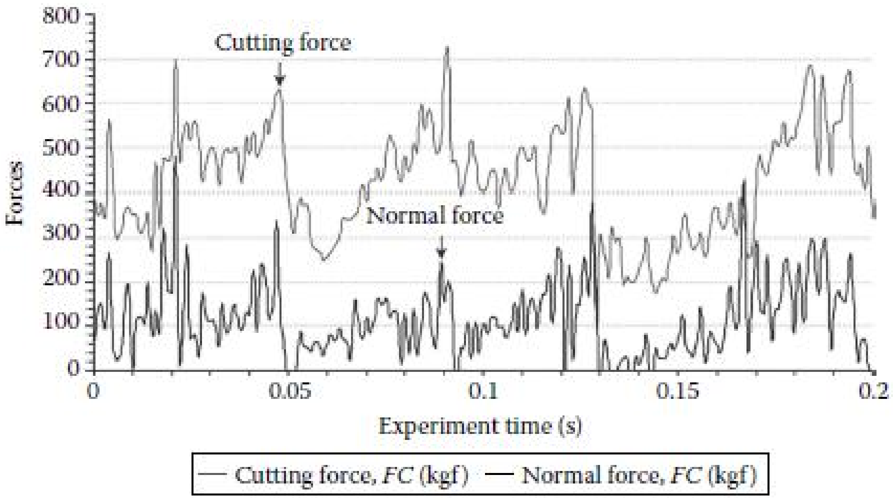


Figure 3-2:Typical recorded forces for chisel cutters while cutting (Bilgin,2013)

### 3.1.2 Radial Cutters And Complex – Shaped Chisel Cutters

In this circumstance, theoretical works have been improved with several simplifications and suppositions and generally for chisel tools and unrelieved cutting mode. Therefore, the theoretical model should be changed due to the different tool dimensions, cutting conditions, flat wear and also front ridge angle and v – bottom angle (Figure.3.3). In this circumstance, theoretical works have been improved with several simplifications and suppositions and, generally for chisel tools and unrelieved cutting mode. Therefore, the theoretical model should be changed due to the different tool dimensions, cutting conditions, flat wear and also front ridge and v – bottom angle. In addition to, the mining equipment which has a rotating cutterhead and which mounts cutting tools in an array where there is always an interaction between the grooves generates a relieved cutting condition (Bilgin, 2013). Moreover, the optimum (s/d) ratio is approximately 2 for chisel and conical cutters when the rock condition is medium – strength (Bilgin, 2013).

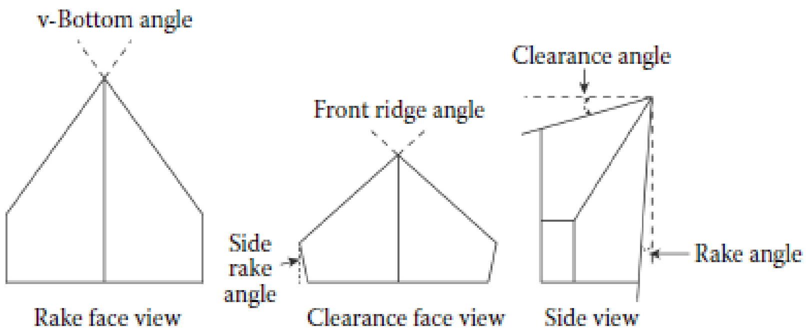


Figure 3-3:Angles Of Complex Chisel Tools (Bilgin., 2013)

$$F'C_w = k_1.k_2.k_3.k_4.\left[\frac{2.\sigma_t.d.w,\sin\frac{1}{2}\left(\frac{\pi}{2} - \alpha\right)}{2 - \sin\frac{1}{2}\left(\frac{\pi}{2} - \alpha\right)}\right]$$

The equation shows Evan's cutting model, which has been reformed by Bilgin (2012) to be used for chisel and complex – shaped cutters by applying some coefficients.

where:

$F'Cw$ ; is a peak cutting force for a worn, complex chisel tools,

$k_1$ ; is a coefficient used for taking into account the effect of wear flat on tool force,

$k_2$ ; is a coefficient used for evaluation of effect of front ridge angle,

$k_3$ ; is a coefficient used for effect of v-bottom angle,

$k_4$ ; is a coefficient used for effect of cutting in relieved mode,

$\sigma_t$ ; tensile strength,

d ; depth of cut,

w ; width of tool,

$\alpha$ ; rake angle (Bilgin et al. , 2013).

Apart from the aforementioned cutter tools, the disc cutters are mostly used in TBM (Tunnel Boring Machine). The following explanations will be devoted in terms of examining the performance analysis of disc cutters, their literature review in terms of empirical, theoretical expressions and a focus on computer-aided modelling of disc cutter analysis.

## 3.2 DISC CUTTER TOOL AND PERFORMANCE ANALYSIS METHODS

The disc cutters are one of the main components of TBM: they are mounted on the TBM cutterhead. They were rigged very early with discs, toothed (chisel, drag and picks) and tungsten carbide insert bit (TCI) (Figure 3.4). According to Maidl (2013), the distance of the cutter trajectory and the diameter of the disc cutters can be chosen according to the characteristics of rock and its cuttability (Maidl et al., 2013). Furthermore, the rotating cutterhead thrust the discs towards the face with high pressure and the tools roll around the tracks in the face. When the applied pressure surpasses the compression strength of the rock and pulverizes it locally, so the discs penetrate the rock until applied pressure and rock strength is in balance. This explanation is known as penetration, and it leads to the large flat chip of rock, shown in Figure 3.5 (Maidl, 2013).

Figure 3-4:: Disc cutter And TCI (Maidl, 2008)

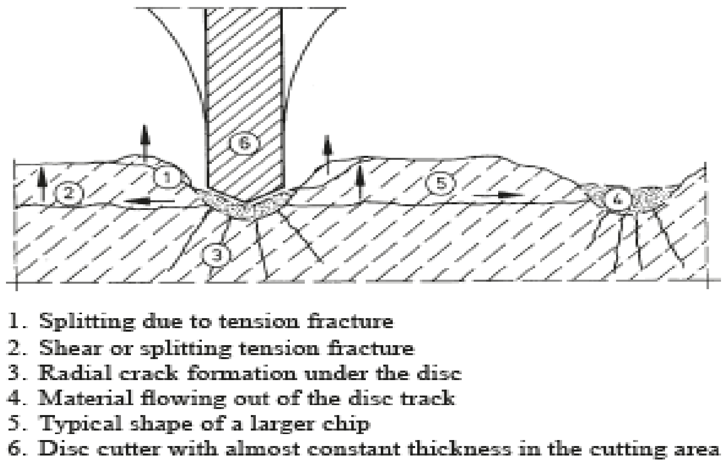


Figure 3-5:Illustration of disc cutter cutting process (Maidl,2013)

Within the frame of the concepts, there are two different theories about the cutting process of disc cutters, which are related to rock spalling and to surrounding roll tracks. The previous suppositions, probably inspired by the wedge section of the discs, presumes a shearing process initiated by the flanks of the disc. According to this basis, the cutting angle has led various authors to different performance assumptions. The typical wear of the discs by material displaced sideways puts not only the shearing theory but also the fundamental influence of the cutting angle into question (Figure 3.6), (Maidl et al., 2008).

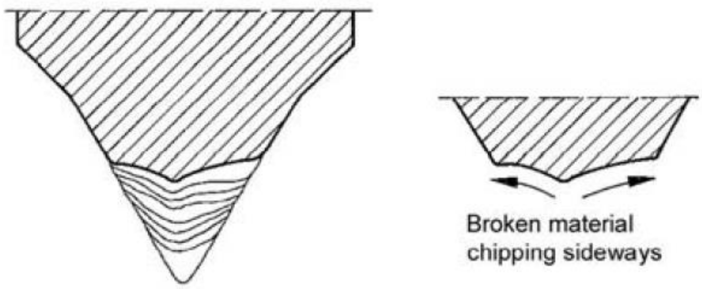


Figure 3-6:Worn state of disc cutter (Maidl et al., 2008)

Newer assumptions, influenced mainly by disc cutters of almost the same thickness in the working area, assume a splitting tension loading preferably, supposing that the penetration reaches values of 4 - 15 mm, in softer rock up to 20 mm or more (Maidl et al., 2008).

Apart from abovementioned scientific knowledge, there are issues considering the roughness of the surface. The roughness occurs by anisotropy and discontinuities, which can cause a high amount of peaks into the disc loading (Maidl et al., 2008). The disc cutter bore, based on the penetration, along 60 – 90 mm of its boundary. It can be easily noticed that minor loading is for 0,025 s called gauge cutter, and also 0,3 s for discs near the centre, enormous peak loads are implemented to both rock and discs (Maidl et al., 2008).

### 3.2.1. Performance of Disc Cutters And Analysis

TBM performance has been influenced by a range of inside and outside parameters, but the disc cutters have one the most impacts on TBM performance. During tunnelling, the discs are worn out due to geological features and properties of the equipment, and in this case, the machine has to be stopped in the middle of the tunnel to avoid disastrous failures. In case of any ruinous break downs, the disc cutters must be changed in scheduled time, but every downtime leads to lost profit and all of these operations cause time losing as well. For these reasons, the disc cutters are improved for specific machine types and sizes, as well as for different geological conditions. For instance, varied dimensions of cutters need a different size of machines such as 19 and 20 inches disc cutters to need a larger TBM. Whatsmore, disc cutters are designed depending on specific geological conditions, for example, for extremely competent rock the most expensive cutter rings are used. In contrast, the same cutter rings have fewer advantages in weaker rock mass condition. As a result, the selection of a proper disc cutter is the most remarkable operation to reduce risk and cost while increasing profit and TBM performance (Roby, 2008).

Performance analysis and prediction models are divided into two main categories, such as thoroughly empirical and theoretical/empirical. In addition to models, last decades computer-aided models such as SPSS software, machine learning methods, are widely used to predict and improve performance not only of the TBMs but also of TBMs components. During the analysis of performance, some regression methods are employed among rock properties, penetration rate, normal force, rolling force and specific energy. Furthermore, two main approaches are widely used in performance analysis of TBM and cutter tools analysis, that are CSM (Rostami and Özdemir, 1993) and NTNU (Listrud 1988, NTH 1995, Bruland et al. 1995). In this regard, several disc cutter performance analysis methods have been developed by various researchers. All mentioned methods will be discussed and examined in terms of empirical, semi-empirical, experimental and also by computer-aided modelling.

### 3.2.2. Analysis of the Friction Process between Disc Cutter and Hard Rock

While TBM advances into the tunnel, cutterhead applies a given pressure to the face through the disc cutters, as previously mentioned. During that operation, disc cutters are exposed to wear due to the rock mass abrasivity, so the cutter life decreases and downtime occurs in a project. Therefore, the wanted penetration is not obtained as the situation causes a too small penetration into the rock and the different abrasion force direction on the cutter tool roughly acts along the cross-section of the rock. Moreover, during the rotation of the TBM cutterhead, the disc cutter rolling line is higher than the penetration depth into the rock. As a result, the vertical force is not taken into account; Figure 3.7 shows those forces acting on the disc tool.

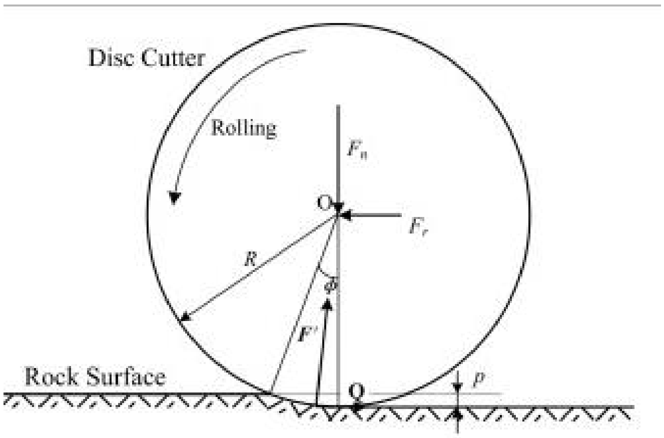


Figure 3-7:Forces acting on the cutter tool (Wen and Ping Huang, 2015)

Fn ; Normal force (thrust force),

Fr ; Rolling force,

F′ ; Normal Rock Reaction,

Q ; Friction force between the disc cutter and the rock,

p ; depth of penetration,

R ; Cutter Radius,

Φ ; Contact surface

Fr (rolling force) is defined as:

$$Fr = F_r' + Q$$

Fn (thrust force) is expressed by:

$$\mathrm{Fn} = \mathrm{F}'_{\mathrm{n}}$$

$\mathrm{F}'_{\mathrm{r}}$ = horizontal component of the rock normal reaction force,

$\mathrm{F}'_{\mathrm{n}}$ = vertical component of the rock normal reaction force,

Q ; Friction force is expressed by:

$$Q = \alpha \,.\, \mathrm{Fn}$$

α ; undefined coefficient so if the rolling force is not enough or weak, $\alpha = 0$, sliding situation is occured, $0 < \alpha < \mu$, and when the rock mass or sample surface is fully sliding, $\alpha = \mu$.

Accoring to (Wen and Huang, 2002), the relationships between friction and wear volume are formulated by:

$$W = E_R \,.\, \Delta V = [mE_b / k(\xi m + 1)] \,.\, \Delta V$$

In this equation, W refers to the friction force, $E_R$ represents the wear energy required per unit volume, $\Delta V$ is the wear volume, $E_b$ is the actual chip formation energy density and m is the critical friction time. k and $\xi$ are coefficients which are associated with material physical properties of both disc cutter and rock (Wen and Ping Huang, 2002).

### 3.2.3. Disc Cutter Performance Analysis Models

#### *3.2.1.1 Fully Empirical Models*

- **Graham (1976)**

In this performance analysis model, disc cutter tools have been examined in terms of each cutter head revolution (rpm) relationship between the function of normal force per cutting and uniaxial compressive strength of the rock. Therefore, the model has been developed for TBM performance which was related to several geological and structural properties at different thrusts per cutter. The following equation expresses the Graham model:

$$P = \frac{3940. F_L}{\sigma_{cf}}$$

$F_L$= average cutter force (kN)

$\sigma_{cf}$= UCS of the rock (kN/m$^2$)

P= penetration per revolution (mm/rev)

- **Farmer and Glossop (1980)**

The performance analysis model is related to the relationship between discs penetration, that is associated with normal force and friction strength of the rock. Eight different TBM data had been evaluated in that model, but the limited number of data was the main reason for the lack of the model. Apart from these, homogenous rock properties, discontinuities and also geometric characteristics had been used. Furthermore, the model was formulated as follows:

$$P = \frac{624.F_L}{\sigma_{tf}}$$

where:

$F_L$= average cutter force (kN)

$\sigma_{tf}$= tensile strength of the rock (kN/m$^2$)

P= penetration per revolution (mm/rev)

- **Nelson (1983)**

The model was conceived on the basis of analysis on tunnels excavated in four sedimentary rock types, and it is expressed as:

$$PR = 10{,}45 - 1{,}19.H_A$$

PR=penetration rate

HA= hardness estimated by Tarkoy & Hendron (1975)

In this model, the penetration rate has been calculated based on thrust and the rock type and also based on the correlation among the rock hardness and the normal penetration, so it has been defined through the following equation in terms of improved thrust:

$$FPI = 5{,}95 + 0{,}18.H_T$$

$$H_T = H_R.\sqrt{H_A}$$

FPI= field penetration index (average thrust on cutter and penetration by revolution ratio) (kN/mm) (lbs/in)

HT= total hardness

HR= Schimdt hammer hardness

- **Bamford (1984)**

The performance analysis model is linked to penetration rate that is related to a linear model based on the Schmidt hammer test, total thrust force, NCB index and friction angle:

$$P = 0{,}535.S - 8{,}49 - 0{,}00344.T - 0{,}000823.N + 0{,}00137.\phi$$

P= penetration rate (m/h);

S=Schmidt hammer rock response;

T= thrust total force (t)

N`= NCB index (N/mm)

ϕ= friction angle

Even though it has a good correlation, some limitation is due to the analysis on single tunnel data, competent rock properties and a few machines parameters.

- **Hughes (1986)**

The model has been derived from the Graham model. It comprises some parameters such as mean normal force, rock UCS and rotation speed of the cutter head. Besides, encountered parts of the cutter tool and radius of the disc. The Hughes equation has been obtained from coal mine experience:

$$PR = \frac{6.P^{1.2}.N.h}{\sigma_c^{1.2}.r^{0.6}}$$

$$PW = 28{,}45.D + 9{,}07.D^2$$

where:

PR= penetration rate (m/h)

P= peripheral cutter force (kN)

N= cutter head rotational speed (rev/s)

h= counterpart cutters

σc= uniaxial compressive strength (kN/m2)

r=cutter radius (m)

PW= power (kW)

D= TBM diameter (m)

- **Barton QTBM Model (2010)**

The Barton model is based on the extended Q system of rock mass classification, and also other parameters are considered, which are average cutter force, abrasivity of the rock and rock stress. By adding new parameters, the QTBM is derived from the function of 20 parameters, and the following formula simplified it:

$$Q_{TBM} = \frac{RQD_0}{J_n} \cdot \frac{J_r}{J_a} \cdot \frac{J_w}{SRF} \cdot \frac{SIGMA}{(F^{10}/20^9)} \cdot \frac{20}{CLI} \cdot \frac{q}{20} \frac{\sigma_1}{5}$$

where:

$RQD_0$ is the conventional RQD,

CLI is cutter life index,

F is the thrust applied on the disc (t)

q is the quartz content,

Jn, Jr, Ja, Jw are the Q index variables evaluated for the most TBM advance direction;

SIGMA; is the rock mass strength,

$$SIGMA_{cm} = 5.\gamma.\sqrt[3]{Q_c}\text{ , where:}$$

$$Q_c = Q_0 \cdot \frac{\sigma_c}{100}$$

$SIGMA_{cm}$ is rock mass strength with unfavorable inclination [MPa],

$\gamma$ is a density,

$\sigma_c$ ; Uniaxial compressive strength

After a long time and a number of projects Barton found a simple equation between penetration and QTBM:

$$\text{PR} = 5(Q_{TBM})^{-0,2}$$

- **The RSR Model (Innaurato et al., 1991)**

Innaurato (1988), (1991) developed a proper correlation between PR (penetration rate), rock structure rating (RSR) and UCS of hard rock:

$$\text{PR} = 40.41UCS^{-0.44} + 0.047\text{RSR}+3.15$$

where:

PR is expressed in mm/round and UCS in MPa. The data set has been implemented by five different tunnel projects within igneous, sedimentary and metamorphic rocks whose UCS was in the range 50 – 150 MPa.

The RSR is associated to RMR:

$$RSR = 0.77RMR+12.4$$

and it has been used by Innaurato to derive RSR while not available.

Furthermore, Innaurato (1991) created two different models as simulated and recorded according to three different rock samples. The model was created as a function of RMR and difference between simulated and recorded values shown in Figure 3.8 (Sapigni et al., 2002).

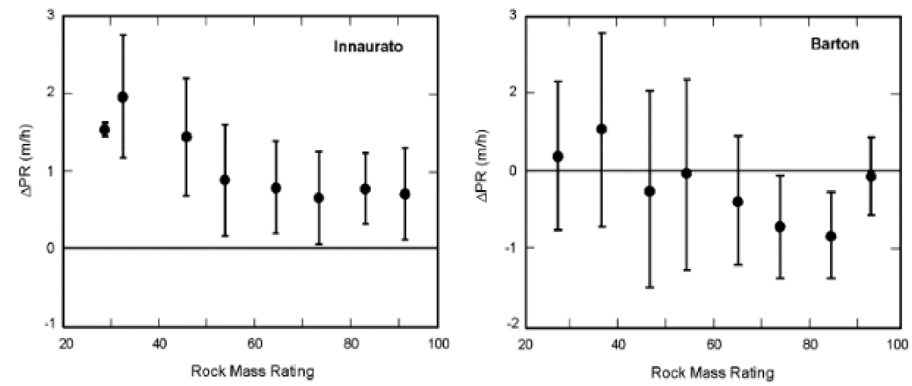


Figure 3-8:Difference between recorded and evaluated penetration rate as a function of RMR. Prediction difference between Innaurato (1991) and Barton (1999) (M.Sapigni et al. 2002)

### 3.2.4. NTH Model or Norwegian Method (NTNU)

The NTNU model refers to Norwegian University Of Science And Technology, and it was the first time published by NTNU ( Norwegian Institue Of Technology, 1976). Furthermore, that model has been modified by Bruland (2000) and Macias (2016).

Assessment of the NTNU model has been obtained from more than 300 km of tunnels and 40 different tunnel projects in terms of performance estimation and cutter span considerations. Apart from the other empirical models, the NTNU is based on the correlation between properties of geological formation/rock mass mechanical specifications and real tunnelling performance. Whatsmore, the preferable version of the NTNU model is (Bruland, 2002) in the sector of the industry. According to Bruland model, the net penetration rate is specified as the forward motion of the TBM when the cutterhead pivot with thrust encounters the face, verbalised in meters per hour (Bruland, 2002; Hansen, 2018).

- **Rock mass fracturing**

In tunnel boring process, rock mass fracturing is the most significant (Bruland, 2000b) among the other parameters, because a less distance in fracturing leads to higher influence on the penetration rate. Moreover, there are three different sorts of fractures, are defined below:

- **Joints (Sp):** they are defined as consistence of fractures surrounding the tunnel section and filled by cohesive or poor materials (Bruland, 2000b; Hansen, 2018)**.**
- **Fissures (St):** they are known as non – continuous joints all surrounding the tunnel profile. They consist of low shear strength or bedding plane fissures (Bruland, 2000b, J.N. Hansen, 2018, M.Sc. Thesis)**.**
- **Homogenous Rock Mass (Class 0):** It is defined as mafic rock mass without any joints or fissures. If the filled joints have high shear strength, they can be categorized as a homogeneous rock. (Bruland, 2000b; Hansen, 2018.

Besides, when creating a mapping for tunnel, Bruland (2000b), created fracture classes to identify weakness plane and it is seen in Figure 3.9.

| Fracture class (Joints = Sp / Fissures = St) | Distance between planes of weakness [cm] | |
|---|---|---|
| O | - | - |
| O-I | 160 | - |
| I- | 80 | 90 |
| I | 40 | 80 |
| II | 20 | 40 |
| III | 10 | 20 |
| IV | 5 | 10 |

Figure 3-9:Fracture class and distance planes of weakness (Bruland, 2000b, J.N. Hansen, 2018, M.Sc. Thesis)

- **Angle Of Orientation (α)**

Apart from the weakness of the plane, alignment of the tunnel axis influences rock mass fracturing and penetration rate. The alignment of the joints which are related to tunnel axis is expressed by the **α** angle and is evaluated by the formula below:

$$\alpha = \arcsin . (\sin a_f . \sin (a_t - a_s))$$

where:

α: smallest angle between discontinuities and tunnel axis

$a_f$: dip angle of the weakness plane

$a_t$: tunnel axis

$a_s$: strike angle of the weakness

Bruland (2000b) has demonstrated relationship between α – angle, fracture class, joints and fracturing factor (ks), as shown in Figure 3.10. (Bruland, 2000b; Hansen, 2018).

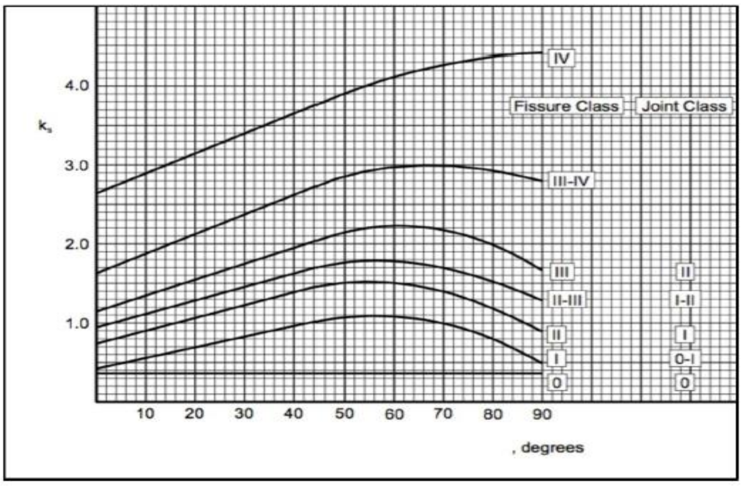


Figure 3-10:Fracturing factor (Bruland, 2000b; Hansen, 2018)

- **Drilling Rate Index (DRI)**

The DRI is obtained by computing the rock hardness or rock drillability and depends on consequence of two kinds of laboratory tests, such as the Brittleness test ($S_{20}$) and the Siever's J – miniature drill test (H.Yenice et al., 2018). Figure 3.11 shows the test and its procedure.

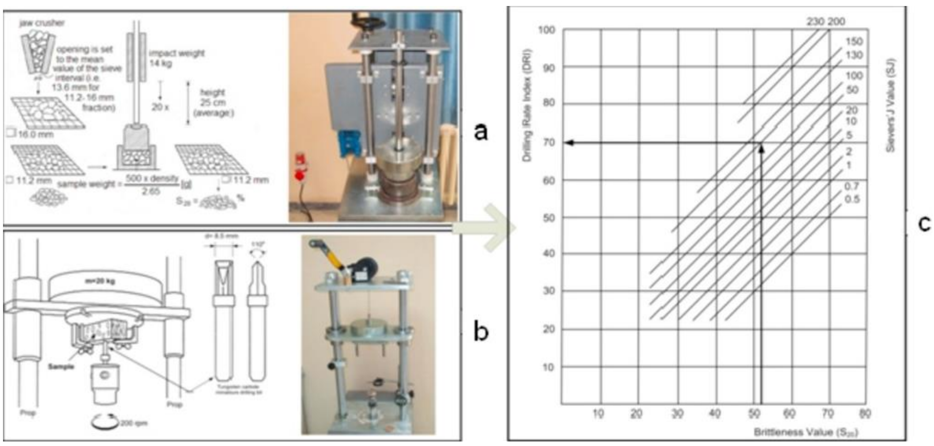


Figure 3-11:Determination of DRI (Dahl,2003)

Through this test, the abrasion value (AV) is defined as the weight loss in 1 mg of tough – metal sample after about 100 rotations when the grain size distribution of the crushed rock sample is lower than 1 mm (Nilsen and Özdemir, 1993).

Another testing method has been sustained as a sub-subject of the NTNU model, and it is called Bit Wear Index (BWI). The BWI is a combination of the DRI and abrasion test. Still, in nowadays performance models of the TBM the test has just been mentioned here because it is essential in terms of comparison of mechanical properties (Nilsen and Özdemir, 1993). In the NTNU model, the procedure of cutter wearing analysis is a bit different from the percussive drilling bit wear, so that in case of cutter tool abrasivity consideration, the abrasion "AVS" is determined. Nilsen and Özdemir, 1993). The "AVS" is explained by utilising test sample made from cutter steel in the abrasion test instead of one made from hard metal. According to laboratory test outcomes, the cutter life index is evaluated by the formula below:

$$\text{CLI} = 13{,}84\ .\ (SV/AVS)^{0.3847}$$

- **Penetration Rate**

(Bruland, 2000b) has described the penetration rate as the advancement of TBM per rotation. The penetration rate is computed by equivalent thrust per cutter $(M_{ekv})$, the critical cutter thrust $(M_1)$, and penetration coefficient (b) respectively. Furthermore, the critical thrust can be evaluated from Figure 3.12 and the penetration coefficient from Figure 3.13. Both figures are seen in the following page.

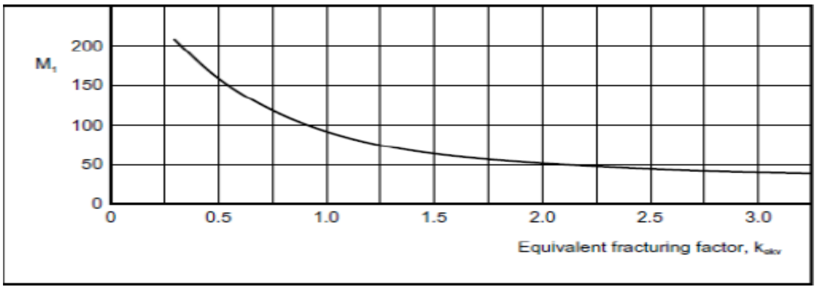


Figure 3-12:Critical thrust as a function of the equivalent fracturing factor (Bruland, 2000b, J.N. Hansen, 2018, M.Sc. Thesis).

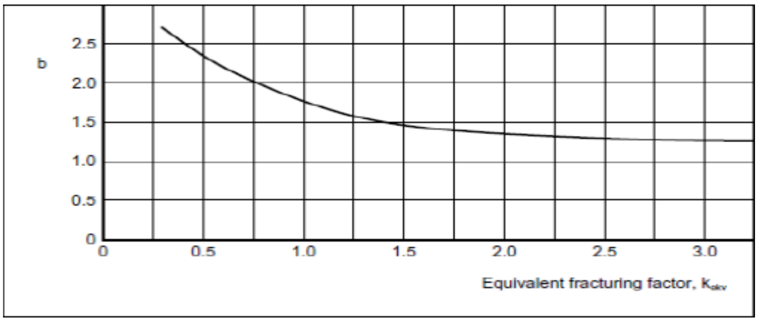


Figure 3-13:Penetration coefficient as a function of the equivalent fracturing factor (Bruland, 2000b; Hansen, 2018).

Penetration rate is expressed as:

$$i_0 = (\frac{M_{ekv}}{M_1})^b$$

where:

$i_0$ basic net penetration rate [mm/rev],

$M_{ekv}$ equivalent cutter thrust,

$M_1$ critical cutter thrust

b penetration coefficient

Net penetration rate:

$$I_0 = i_0 \ . \ RPM \ . \ (\frac{60}{1000})$$

Where:

$Io$ basic net penetration rate [m/h]

$io$ basic penetration rate [mm/rev]

$RPM$ cutterhead velocity [rev/min]

### 3.2.5. Theoretical Empirical Models

- **Roxborough and Phillips**

In this model, five different parameters have been evaluated, i.e. diameter, penetration, sharpness angle, cutting speed and spacing. Apart from spacing, other variables are considered by single continuous disc operations but spacing includes a decision of the optimum distance among the tools in a lay out (Roxborough and Phillips, 1975).

According to (Roxborough and Phillips,1975), the disc cutters are affected by their geometry, as shown in Figure 3.14, and rock mass strength properties. The principle of the disc cutters is expressed and formulated according to a simple mechanism. When penetration increases, chord length (*lenght of the arc contact*) which has relationship between disc/rock contact and center of the disc is formulated by the following equation:

$$l = 2\sqrt{Dp - p^2}$$

D: diameter

l: chord length, (Length of the arc of contact)

p: depth of cut

In addition to these, another equation is related to the area of contact of the disc:

$$A - 2pl \, . \tan\frac{\Phi}{2}$$

Final formulation is associated with the thrust equation:

$$F_T = 4\sigma \tan\frac{\theta}{2}\sqrt{Dp^3 - p^4}$$

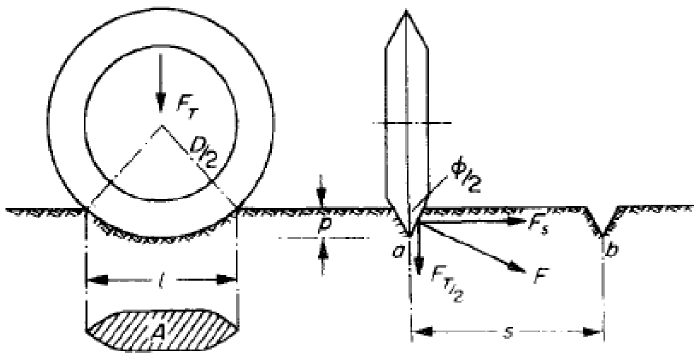


Figure 3-14:Geometry of disc penetration (Roxborough and Phillips,1975)

Figure 3.15 demonstrates a disc under the action of the two principal forces FT and FR. As long as the disc is free rolling and neglecting friction, then the line of action of the resultant R must pass through the centre of rotation to satisfy the zero net torque condition. (Roxborough and Phillips,1975).

$$F_R.\overline{of} = F_T.\overline{oe}$$

so that

$$\frac{F_T}{F_R} = \cot\psi$$

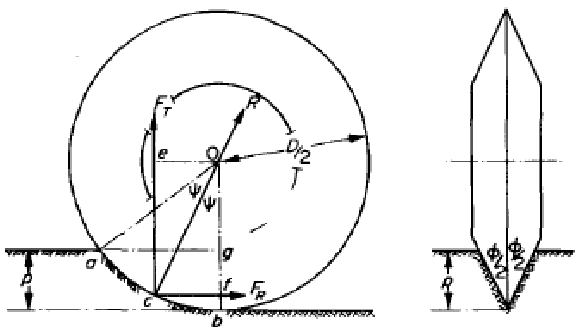

Figure 3-15:Orthogonal Forces Acting On A Disc (Roxborough and Phillips,1975)

As a consequence the rolling force is:

$$F_R = 4.\sigma.p^3.\tan\frac{\phi}{2}$$

- **Rostami and Özdemir Model**

Rostami and Ozdemir (1993) and Rostami et al. (1996) presented a model dependent on the pressure distribution along the outer boundary of CCS (Figure 3.14), (Constant-Cross-Section Disc Cutter), disc cutters in contact with the rock. Unlike the CCS, V cross-sections have not been used for a long time due to irregular wear on the cutter tips, which gradually change the contact area with the rock. The equations acquired by the mean normal (thrust) force and rolling force were based on the angle of contact between the rock and the disc cutter, the radius of the disc cutter, the width of the disc tip, line spacing between the disc cutters, UCS of the rock, BTS (Brazilian tensile strength) of the rock, and penetration of the discs per revolution of the cutterhead. Related equations are seen in the below :

$$\vartheta = cos^{-1}\left(\frac{R-p}{R}\right) \qquad P_0 = \mathrm{C}.\sqrt[3]{\frac{\mathrm{S}}{\vartheta\sqrt{\mathrm{R.T}}}}\sigma_c{}^2.\sigma_T$$

$$\mathrm{F_T} = \frac{\mathrm{P_0}.\vartheta,\mathrm{R.T}}{1+\vartheta} \qquad \mathrm{FN} = F_t.\cos(\vartheta/2) \qquad \mathrm{FR} = F_t.\sin(\vartheta/2)$$

where:

Ft: total outcoming force

R: radius,

T: width of the disc,

ϑ: angle of contact between rock and disc,

$P_0$: pressure of crusched zone,

$\sigma_T$: tensile strenght,

C: 2.12,

S: spacing (Bilgin,2013; Rostami and Özdemir 1993)

FN: Normal Force

FR: Rolling Force

- **Colorado School Of Mines (CSM) Model**

Levent Özdemir unveiled the performance analysis and prediction model in 1997. The CSM model has been performed to analyze the penetration depending on laboratory tests at the Earth Mechanics Institue in Colorado, Golden. The outcome of the tests has been correlated to the TBM field tests due to include practical results. In the same year, J.Rostami came up with new ideas about modification of the CSM model in terms of new variable equations and new input data related to the cross-section of cutters. The primary philosophical system of the CSM method is related to specific cutter forces to evaluate the total thrust, torque and power needed to the cutterhead. To analyze the performance of the disc cutter in this model, the full-size cutting test was done in various areas which consisted of rock samples, and each test was evaluated the cuttability of rock by using rock strength, toughness and cutting pattern. The performance analysis based on the V – profile type disc cutter. Still, the cutter tool has been modified for industry and also several past theories extracted from wedge indenture into stone have been utilized as a guide. In addition to these, this analysis was used as a guide to determine the incidence of the highly stressed excavated area, and radial stress cracks due to the penetration into the stone sample, seen in Figure 3.16 (Özdemir, 2003; Hansen, 2018).

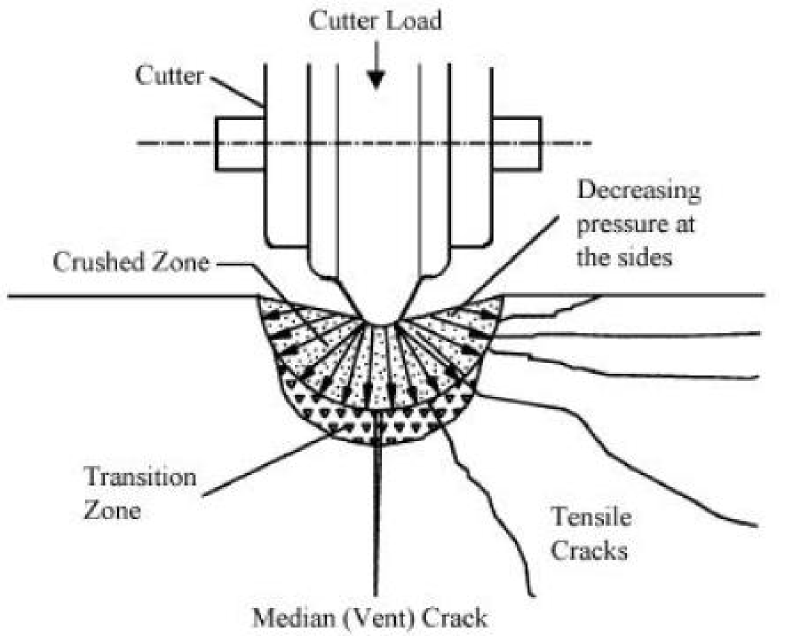


Figure 3-16:Stress fields and fractures under the penetrating edge of the disc cutter.( Özdemir,2003)

- **The CSM Model by Rostami**

In order to define some parameters which are related to disc angle, pressure of the contact area and total force can be computed by the equation that is seen in the below, and also contact area between a rock and a disc cutter are shown in Figure 3.17, (Hansen, 2018):

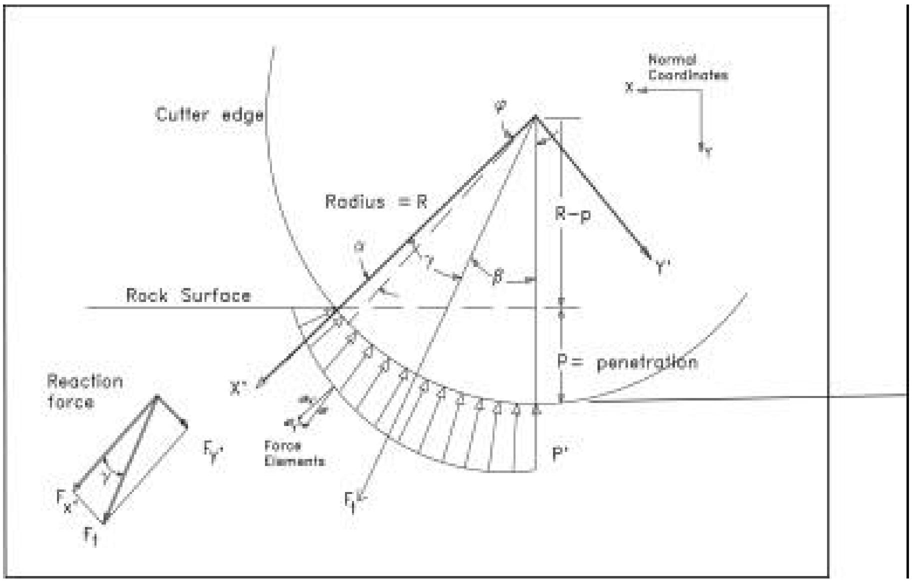


Figure 3-17:Force on a disc cutter in the CSM Model (Rostami, 2013)

$$\Phi = \ cos^{-1}(\frac{R-P}{R})$$

where:

Φ: angle of contact,

R: cutter radius,

P: penetration rate,

$$P^0 \ = C * \sqrt{\frac{S * \ \sigma_u^2 * \sigma_t}{\Phi * \ \sqrt{R * T}}}$$

where:

$P^0$ : pressure of contact area,

C : cutting coefficient,

S: spacing of cutters,

$\sigma_t$: brazilian tensile strength,

$\sigma_u$: UCS,

T: cutter tip width

Another formula is used to find the total thrust:

$$F_t = \left( \frac{T * R * \Phi * P^0}{(1 + \Psi) * 1000} \right)$$

where:

$F_t$ : total thrust per cutter

Ψ: stress distribution factor

Finally, after having calculated the total force, normal and rolling force are evaluated by the following formulas :

$$F_n = F_t * \cos ( \Phi / 2 )$$

$$F_r = F_t * \sin( \Phi / 2)$$

where:

Fn: normal thrust per cutter,

Fr: rolling force per cutter,

As a consequence of the CSM model by Rostami, total requirement force, torque and rotational speed are calculated by the following formulas:

$$Th^* = \sum_{1}^{N} F_n \approx N * Fn$$

$$Tq^* = \sum_{1}^{N} F_r \approx 0{,}3 * D * N * Fr$$

$$\text{RPM} = \frac{V}{\pi * D}$$

$$P^* = \frac{\pi}{30} * Tq^* * RPM$$

$Th^*$: total thrust requirement,

$Tq^*: total\ torque\ requirement,$

D: TBM diameter,

N: number of cutters,

RPM: rotational speed (rev/mm),

V: linear velocity of the cutter,

$P^*$: power requirement ( Hansen, 2018).

# 4 CHAPTER – 4

## 4.1 COMPUTER AIDED MODELLING PERFORMANCE ANALYSIS METHODS

CAM (computer-aided modelling) is defined as using different software, programming and algorithm to analysis cases and problems to get proper information about employed operations. The CAD is prefered to avoid uncertainties during engineering applications because theoretical and empirical models are not sufficient to minimize uncertainties of the dataset. Moreover, computer-aided models can work with many input data. In contrast, theoretical or empirical models have some constraints in terms of the high amount of input data. Therefore, the CAD models such as machine learning applications (ANN, Deep Learning, AI) and statistical models that are SPSS (IBM SPSS) operated in last decades in TBM performance analysis and prediction for the future tunnelling operations.

Related to the abovementioned concepts, several CAM models will be explained in terms of TBM and disc cutter performance analysis in the following pages.

### 4.1.1 K – Nearest Neighbor (KNN)

The KNN is a kind of supervised learning model, but it is a kind of non- parametric model that has been commonly performed to statistics for the early 1970s. The KNN is one of the most preferable in data mining due to its effectiveness, simplicity and applicability. The KNN model can apply real-world classification tasks such as expert and intelligence system. The KNN model works with the categorisation of k samples which are defines as similarities between the dataset. By using k sampling, the distance between points on a graph can be computed. Furthermore, the KNN model is used to predict the TBM penetration rate. The model also decides the k number of unknown data among the evaluation of the average samples (Xu et al., 2019).

### 4.1.2 Support Vector Machines (SVM)

SVMs is one of the preferable methods for clustering and regression analysis. The model is implemented for incredibly dimensional (very high number of the dataset) and non – distinguishable datasets. The SVM is based on statistical learning theory, and the primary purpose of the SVM classifier is to define an adequate allocation hyperplane which can divide two classes. Moreover, the method is significantly useful to reduce error and complexities (Xu et al., 2019).

### 4.1.3 Artificial Neural Network (ANN)

The ANN is a mathematical model, but it is different from the other methods in terms of working principle. The working principle of the ANN looks like neuron systems in the human body, and its function is operated as a biological neural network system by using a sigmoidal activating procedure. The ANN technique is utilized to make decisions among the non – linear relationships. In addition to these, the ANN can figure out model interaction between dependent and independent values. The ANN is employed to perform data processing, classification and function estimation (Xu et al., 2019). Figure 4.1. shows an example of an ANN determination structure.

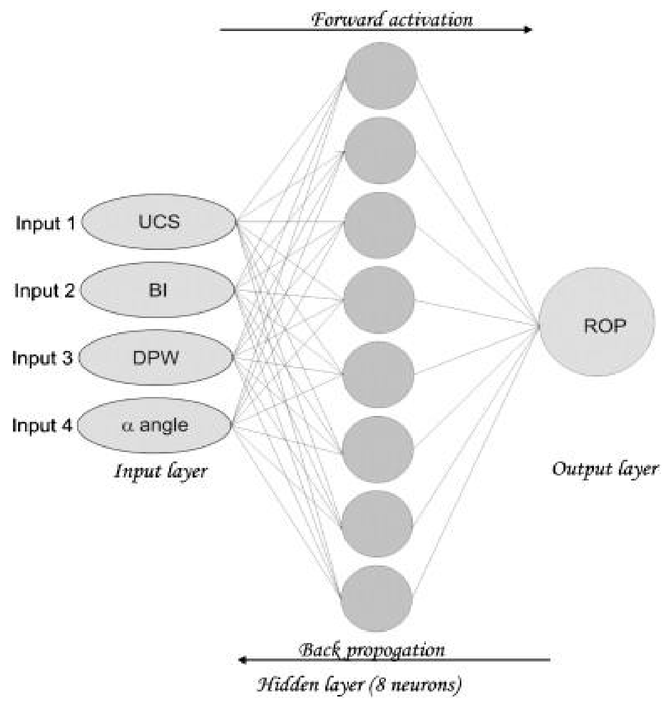


Figure 4-1:Structure of ANN model (Yagiz,2009)

### 4.1.4 Classification And Regression Trees (CART)

The objective of the CART techniques is applied to determine the best likelihood split. Among the multifold input values, the CART classifies the data in terms of the smallest and largest values. The CART is also called decision tree due to it creates flowchart like the tree. In the CART model, each outcome behaves like a branch of the tree, and each leaf acts as a class label. The CART model is easier for interpretation and more accuracy. Therefore, when it is applied for TBM projects, it will provide more accurate results.

### 4.1.5 Chi-Squared Automatic Interaction Detection (CHAID)

The model is a kind of tree-type (flowchart) structure method that is a group of the rule categorisation. The CHAID provides a tree (flowchart) model of the dependent variable to estimate the independent values. The technic tries to create more extension and non-binary trees (flowchart which has tree structure) Basically, it measures connection of dependent and independent variables (Xu, et al, 2019).

### 4.1.6 Non – Linear Multiple Regression Analysis

The analysis is performed to non – linear relationship between geomechanics engineering/engineering geology and TBM performance models. In this circumstance, different software is utilized, such as R programming language and SPSS software to apply multivariable non –linear regression analysis. Using these depending on the TBM performance dataset, to estimate the most available combination of rock mass parameters in terms of the penetration index (FPI) are considered within the following formula (Salimi et al., 2106):

$$\text{FPI} = e^{(a+b\ .lnUCS+c.lnJs)} = e^{0,868}.UCS^{0,193}.Js^{0,366}$$

where:

FPI: field penetration index,

UCS: Unixial compressive strength,

Js: joint spacing,

An example result of non – linear multiple regression analysis is seen in Figure 4.2.

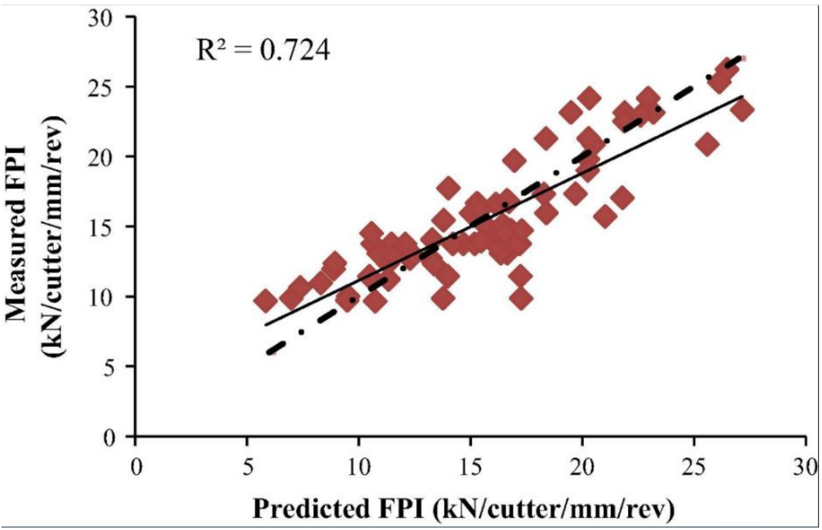


Figure 4-2:Example of relationship between estimated FPI from the multi – nonlinear regression analysis (Salimi et al., 2106)

The main idea of the multi non-linear regression analysis and ANN are based on TBM tunnelling experience and determine dataset according to tunnel experiences. The input parameters consist of geological variable and machine properties, but the most critical parameters are the site conditions and rock mass properties while analysing the TBM performance by using these two techniques (Salimi et al., 2106).

### 4.1.7 Neuro – Fuzzy Modelling Approach

The model has been combined with the fuzzy logic and artificial neural network, and also it has been a popular trend in performance analysis in the last decades. During that process, the ANN (artificial neural network) can supply identification of the pattern and modify the changing environment. At the same time, the fuzzy logic (a kind of logic system) benefit from experiences to reduce uncertainties. As all abovementioned literature, rock mass properties, geology, geotechnical approach, operator and many inside and outside effects have to considered to get the best performance analysis and prediction.

Therefore, in this circumstance, the neuro-fuzzy model approach is suitable, as shown in Figure 4.3 (Alveraz et al., 2000).

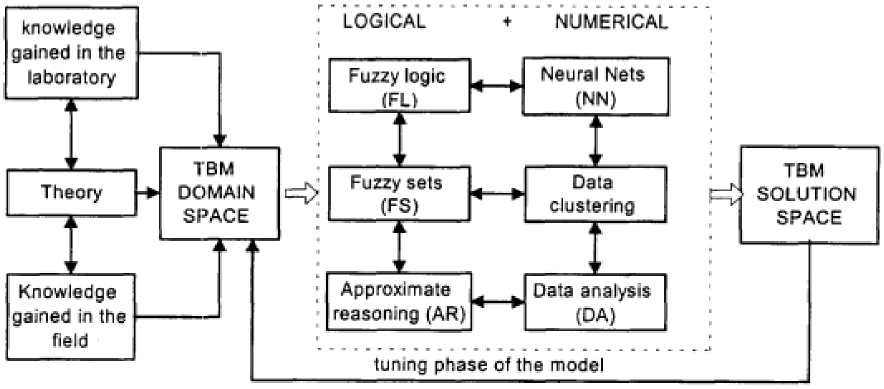


Figure 4-3:Neurofuzzy modeling approach in TBM performance analysis (M.Alveraz et al,2000)

In the TBM tunnelling projects, the PR (penetration rate) is a critical parameter in performance analysis due to impacts the total time to finish the tunnel. The following figure 4.4 shows the penetration rate model, which is used by neuro-fuzzy. The technique has an adequate high database and also allows to analyze the uncertainties of the samples (Alveraz et al.,2000).

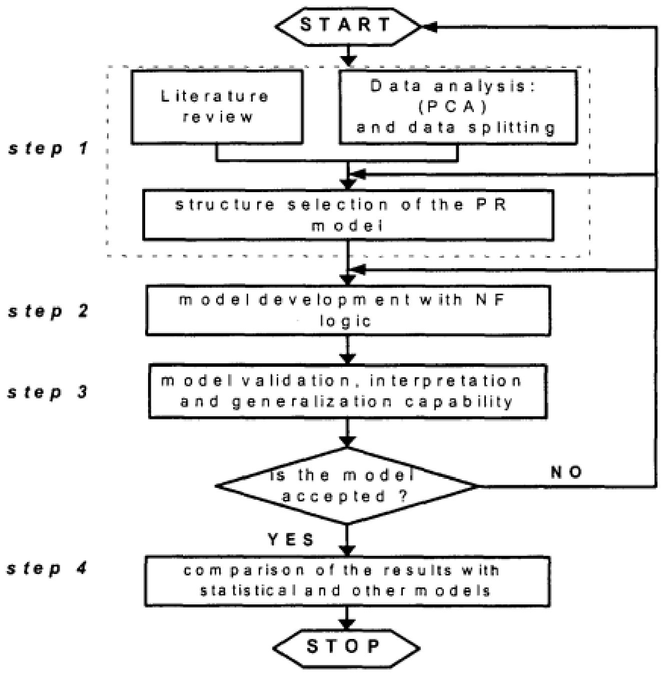


Figure 4-4:Neuro fuzzy algorithm for penetration rate (M.Alveraz et al,2000)

#### 4.1.8 SPSS Analysis

According to Torabi et al.(2013), the penetration rate has been considered as a dependent value. In contrast, other parameters such as UCS, friction angle, Poisson's ratio, cohesion have been evaluated as independent values by using SPSS software. The SPSS is a useful statistical software to linear analysis regression between the parameters as mentioned above to produce a linear equation among the specified values. According to the outcome of the SPSS, the following equation has been obtained for the analysis of the penetration rate in terms of performance:

$$PR = 21.659 - 0.042\,\sigma_c - 0.545C - 0.166\varphi - 31.261v$$

PR: penetration rate

$\sigma_c$: UCS (MPa)

C: cohesion (MPa)

$\varphi$:friction angle

v: Poisson’s ratio

Torabi et al. (2013) proposed a different model for TBM performance analysis, in terms of management, holidays, maintenance and shift change. These parameters state the utilisation factor by using SPSS formula, seen in the below :

$$U = 57.983 + 0.0103T_{exc} - 0.103T_w - 0.067T_h$$

where:

U: utilization factor,

$T_{exc}$: excavation time in hours

$T_w$: wasted time in hours,

$T_h$: holiday time in hours,

Furthermore, the utilization factor parameters are seen in Figure 4.5.

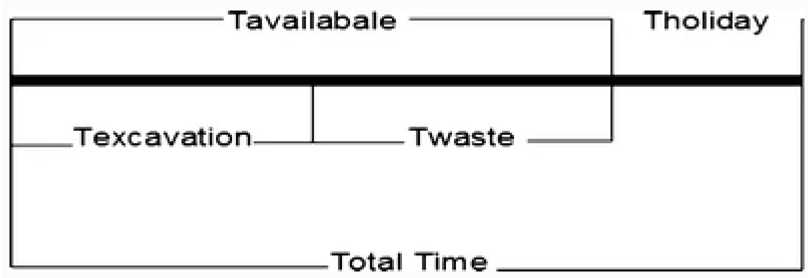


Figure 4-5:Time adjustment of excavation monthly (S.R. Torabi et al, 2013)

According to all the abovementioned techniques, a high number of input data can be evaluated primarily by non – linear relationship. After that, the relation between operation time, downtime and operational cost are computed so the next project will be done by adequate excavation time.

According to all the abovementioned techniques, a high number of input data can be evaluated primarily by non – linear relationship. After that, the relation between operation time, downtime and operational cost are computed so the next project will be done by adequate excavation time.

# 5 CHAPTER – 5

## 5.1 LCM (FULL SCALE LINEAR CUTTING MACHINE)

The full-scale linear cutting machine is commonly used to measure forces which are acting on the cutter tools during excavation. It is the most reliable and correct method for TBM cutterhead design and performance estimation because it can provide practical rock cutting force and efficiency for the determination of cutter spacing, cutterhead thrust, torque and power. The test machine is shown in Figure 5.1. In the testing process, the CCS (constant cross-section disc cutter) and block rock samples, up to 1.0 × 0.7 × 0.7 m sizes, are used. Furthermore, to record normal (thrust) force till 500 kN, a dynamometer is used, and to measure the cutter forces which are into the three vertical directions, a data acquisition system is employed. The acquired data is evaluated for determination and design of mechanical excavator, proper cutting geometry and estimation of performance ( Pan et al, 2019;Balci, 2009).

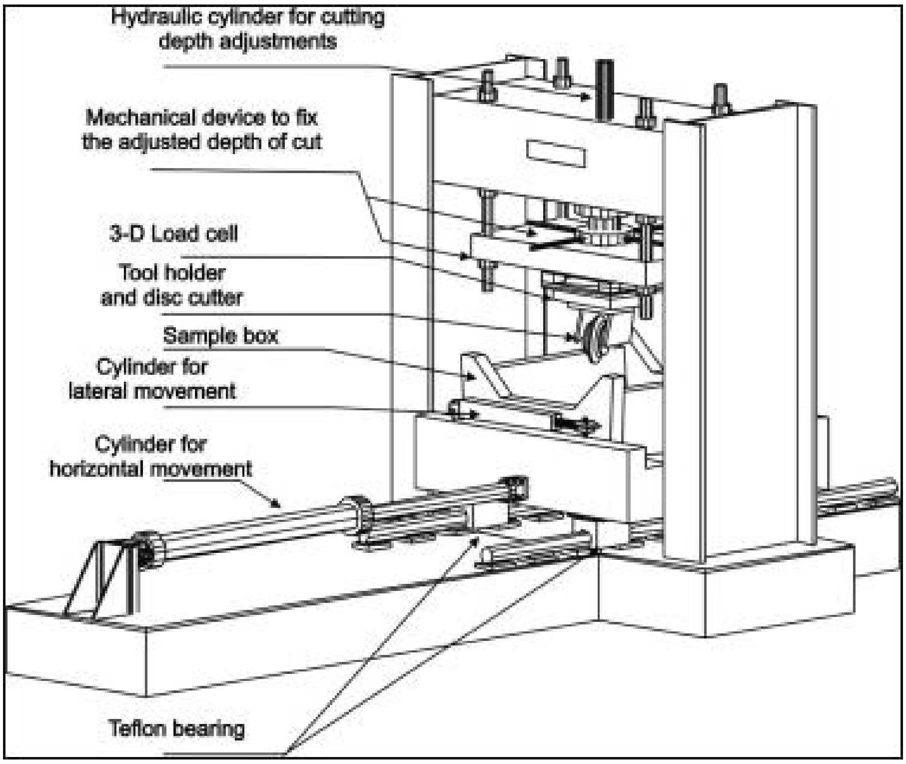


Figure 5-1:The schematic view of the LCM  (Balci, 2009)

Besides, during an LCM test, two main forces are acting on the cutters, and they are called thrust (normal) force and rolling force, shown in Figure 5.2. The normal force is recorded by the machine to compute the thrust requirement of the machine. The rolling force is calculated the torque and power requirement for excavating the rock. The rolling force is entirely associated with torque requirement and used for specific energy calculation.

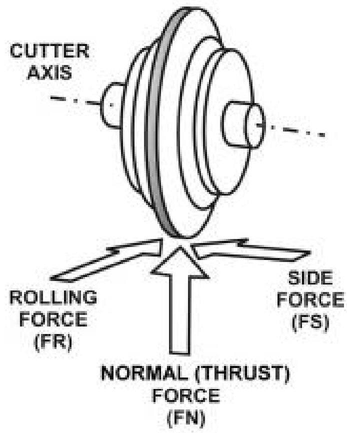


Figure 5-2:The schematic view of the LCM (Balci, 2009)

To calculate the results of the full-scale linear cutting test, the CSM model is employed, which was provided by Özdemir & Rostami (1993) as a semi – theoretical model. Furthermore, the following equations are used to predict analyzes of the disc cutter performance while using LCM (Pan et al., 2019):

Ψ = 0.3714 – 0.0229 . T, has been proposed by Pan et al.(2018)

$\varphi = \arccos\left(\frac{R-p}{R}\right)$

$P^0 = C\sqrt{\frac{s.\sigma_c^2.\sigma_t}{\varphi.\sqrt{R.T}}}$

$$FT_{Rost} = \int_0^{\varphi} T.P^{\theta}.R.d\theta = \int_0^{\varphi} T.P^{\theta}.\left(\frac{\theta}{\varphi}\right)^{\Psi} R.d\theta = \frac{P^{\theta}.R.T.\varphi}{\Psi + 1}$$

$\beta = NRF_{Rost} \cdot \varphi = 0.5000 \cdot \varphi$

$CC_{Rost} = \frac{FR_{Rost}}{FN_{Rost}} = \tan(\beta)$

$FN_{Rost} = FT_{Rost} . \cos(\beta) = FT_{Rost} . \cos(NRF_{Rost}.\varphi) = \frac{1}{\sqrt{CC_{Rost}^2+1}} . FT_{Rost}$

$FR_{Rost} = FT_{Rost} . \sin(\beta) = FT_{Rost} . \sin(NRF_{Rost}.\varphi) = \frac{CC_{Rost}}{\sqrt{CC_{Rost}^2+1}} . FT_{Rost}$ (Pan et al., 2018)

R: disc cutter radius

T: disc cutter tip width

S: cutter spacing

p: penetration rate

σc: UCS

$\sigma_t = BTS\ (Brazilian\ tensile\ strenght)$

Ψ: pressure distribution constant

Φ: contact angle, as shown in Figure 5.3

$P^0$ = pressure under the disc cutter

$P^\theta$ = pressure function and rock cutting contact angle

$\beta$ = angle of the disc cutter result force

$FR_{Rost}$ = disc cutte resultant force

$FN_{Rost}$ = normal force

$FR_{Rost}$ = rolling force

$NRF_{Rost}$ = normalized resultant force

$CC_{Rost}$ = cutting coefficient, (Pan et al, 2018).

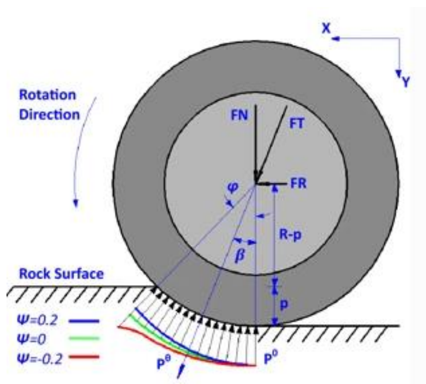


Figure 5-3:Rock cutting contact angle Φ (Pan et al, 2018)

### 5.1.1 Cutter Geometry And Spacing

According to Entacher et al. (2019), th simple penetration function is prevailing for 17” (215,9 mm) disc cutter diameter, tip width T = 19 mm and spacing = 80 mm. The geometry is shown in Figure 5.4.

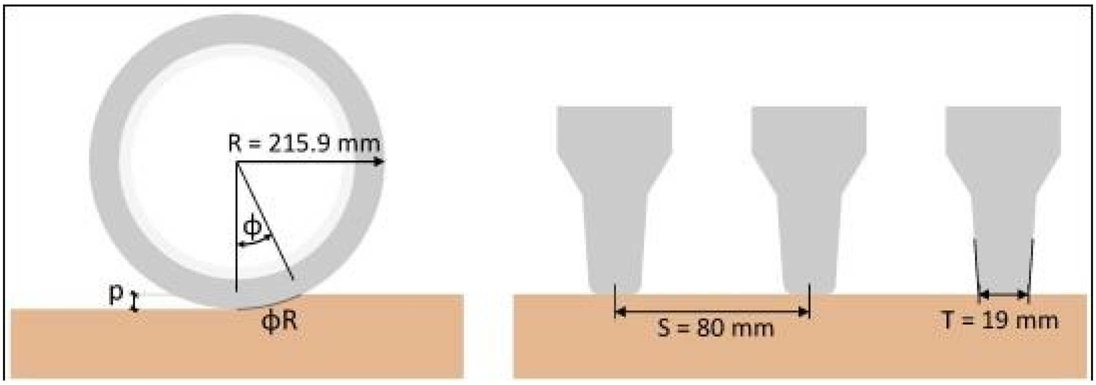


Figure 5-4:Disc cutter dimensions and spacing range (Entacher, 2019)

In the CSM model, there is a parameter which is expressed as a $f_0$ which impacts the cutter spacing as a first term of the model. It is evaluated by dividing the real distance by the indication distance of 80 mm. The formula is given below: :

$$f_0 = \left(\frac{S}{80}\right)^{1/3} . \left(\frac{RT}{4102} C\right)^{0,85}$$

where:

R = diameter

T = width

S= spacing

C = 1 for a 17″, c = 0.946 for a 19″ and c = 0.921 for a 20″ disc cutter respectively.

### 5.1.2 Specific Energy

The specific energy (kN/m$^3$) is known as the amount of energy needed to excavate a unit volume of the rock mass. The SE value is computed by the forces acting on disc cutters, and the forces on disc cutters are predicted by utilizing TBM operation parameters. Besides, the specific energy is directly related to s/p ratio ( spacing and penetration) because to acquire optimum energy for the TBM, appropriate s/p value is required. The relationship between specific energy and s/p ratio is provided in Figure5.5 (Balci, 2009; Pan et al., 2018).

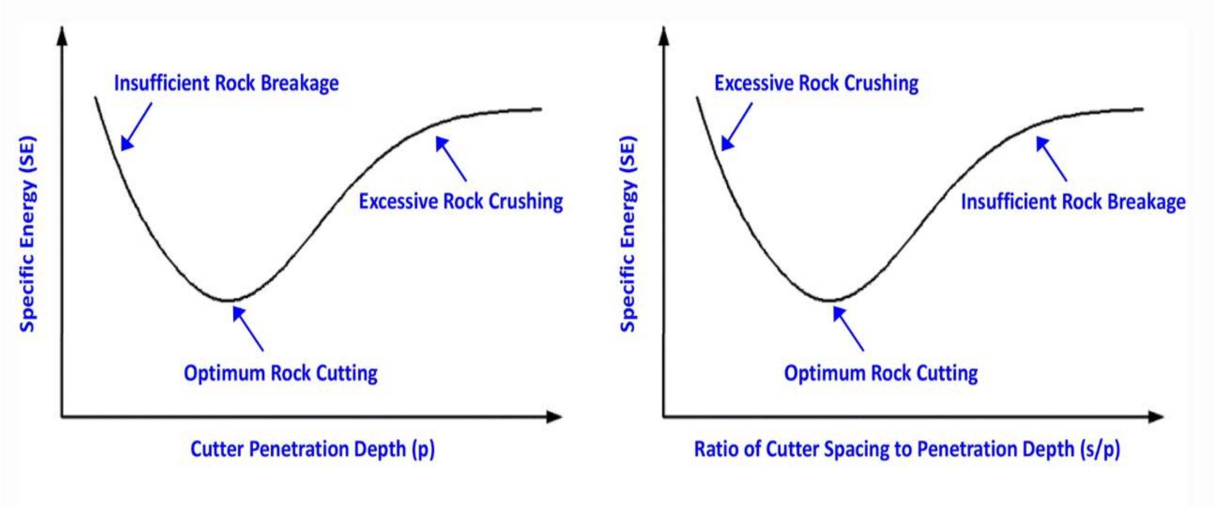


Figure 5-5:Specific energy with cutter penetration depth and the ratio of the cutter spacing to penetration depth (Pan et al, 2018)

According to Balci & Bilgin (2007), the specific energy is expressed by the following formula:

$$SE = \frac{F_R}{Q}$$

where:

$SE$ = specific energy (MJ/m$^3$)

$F_r$ = rolling force (kN)

$Q$ = yield per unit length of cut (m$^3$/km)

Another approach has been provided by Chang et. al (2006) depending on cutting volume, as shown below :

$$SE = \frac{F_r}{P.S}$$

where:

$D$ = rolling force

$P$ =penetration depth

$S$ =cutter spacing

#### 5.1.3 Cutting Coefficient (CC)

The cutting coefficient is defined as the ratio between normal force and rolling force as a percentage. The CC is evaluated as an index of the amount of torque required for a given amount of thrust. It means that if the CC is higher, the TBM requires a higher amount of torque (Hongsu Ma et al., 2016) (Gertsch et al., 2007). Moreover, when penetration increases, the cutting coefficient increases slight linearly (Figure 5.6). The increased penetration is also defined as the correlation between rolling force and normal force, which increase with penetration. The following figure 5.6 shows the relationship between cutting coefficient and cutter penetration (Gertsch, 2007).

The CC is also applied to predict the TBM performance by evaluating the relationship between the rolling force and the normal force (Gertsch, 2007).

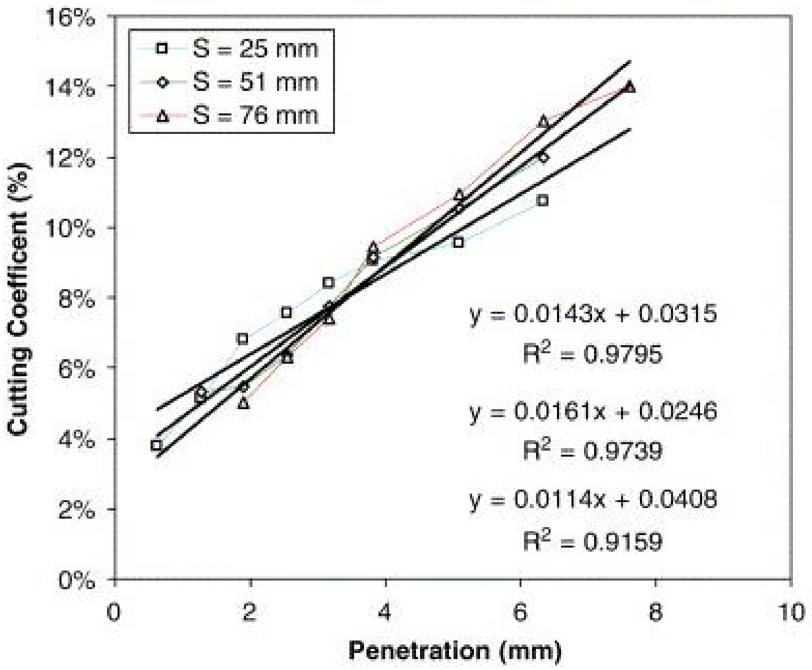


Figure 5-6:Correlation between CC and cutter penetration (Gertsch,2007)

### 5.1.4 Instantaneous Cutting Rate (Net Cutting Rate) (ICR)

The ICR is obtained by the duration of mechanical excavation except for downtime and it is estimated by the following formula :

$$ICR = k.\ P_{net}\ /\ SE_{opt}\ \text{(Bilgin et al, 2016)}$$

where:

ICR = instantaneous cutting rate ($m^3/h$),

$P_{net}$ = cutterhead power (kW),

$SE_{opt}$ = optimum specific energy (kN/$m^3$),

k = energy transfer coefficient ( it is considered 0.8 – 0.9 for TBM ),

The ICR is based on linear cutting test (Bilgin et al, 2016) and the relationship between ICR and net cutting test are shown in Figure 5.7.

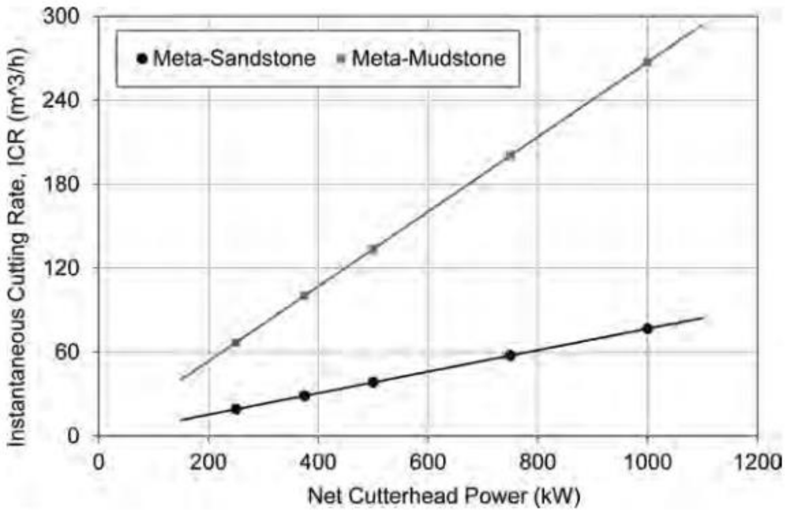


Figure 5-7:Relationship between ICR and Net Cutterhead Power (Bilgin et al.,2016)

## 5.2 INTERMEDIATE LINEAR CUTTING MACHINE (ILCM-POLITECNICO DI TORINO, ITALY)

The ILCM (Figure 5.8), has been developed by Politecnico di Torino, Italy (DIATI) and Institute of Environmental Geology and Geoengineering of the National Research Council (CNR-IGAG). The primary purpose of the ILCM test allows making a test with transportable and available samples (0.5 x 0.3 x 0.2 m). To cut side by side grooves on the same surface of the sample without undergoing edge effect needs mini-disc cutter which has a smaller size than the LCM's disc cutter size for implementing tests with lower penetration (2 - 4 mm). Furthermore, using the correction factor, the results which are taken from the mini disc can be adapted to the real work site in the same machine for the large size cutter tools (Cardu et al., 2017).

Furthermore, ILCM is more usable and affordable than LCM. The other advantages of ILCM tests are handling, positioning and the easy availability of the specimens (Cardu et al., 2017).

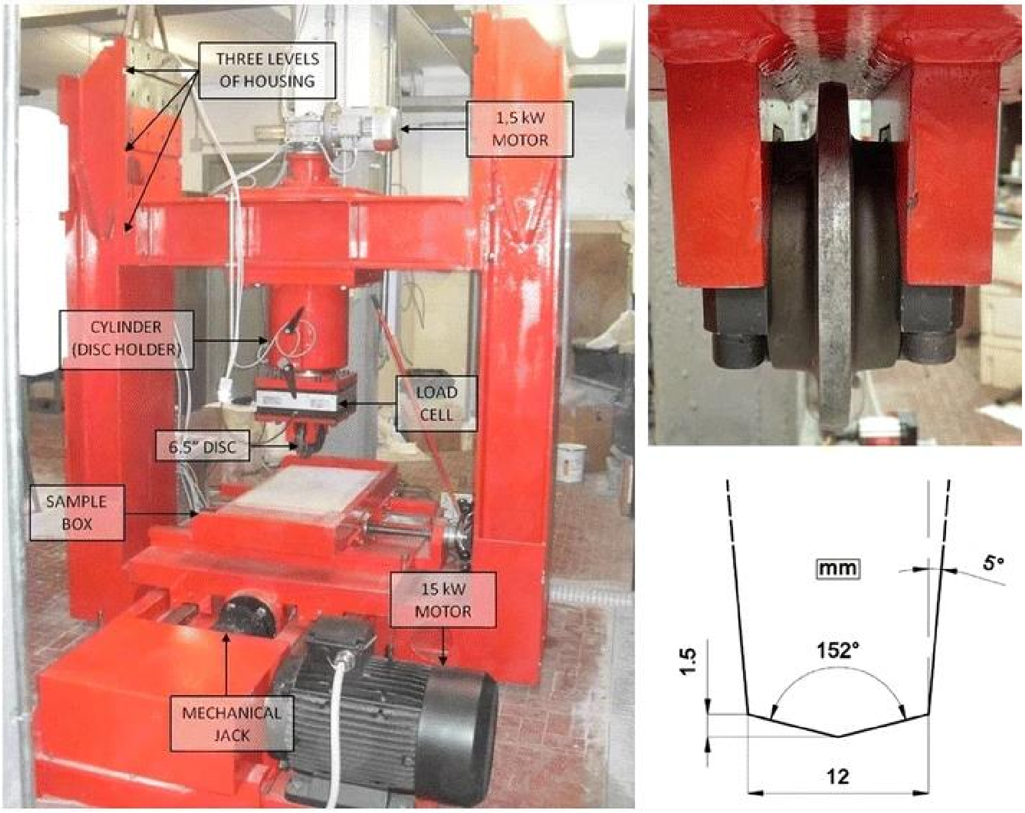


Figure 5-8:ILCM and main components and mini – disc cutter geometry (Cardu et al, 2017)

### 5.2.1 Components of ILCM

To provide enough rigidity and durability of the frame during the tests, the structure of the ILCM includes two perpendicular steel HEB beams (Fig. 5.8).

The structure where is the tool is positioned consists of a cylinder containing a piston which continues the support for the disc and arranges its perpendicular movement for setting the spacing. Using a 1.5-kW electric motor which acts on an eternal (endless) screw (stroke 300 mm); between the base of the piston and the tool, the holder has been mounted a triaxial load (Figure 5.9) cell to consider the three components of the force acting on the disc.

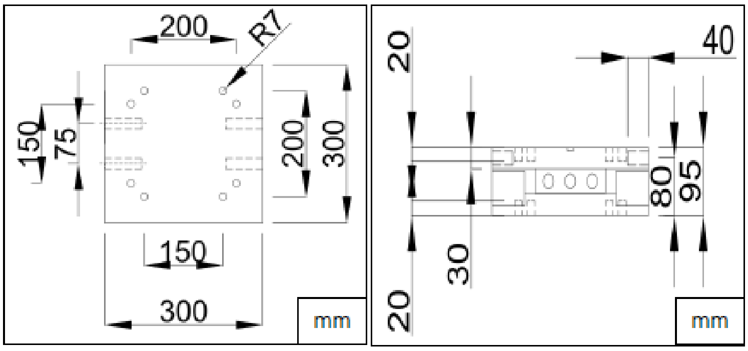


Figure 5-9:Transversal view of triaxial load cell (Rispoli, 2013)

Other technical properties of the ILCM are expressed by the following list:

- Capacity of X and Y direction = 100 (kN)
- Capacity of Z direction = 200 (kN)
- Disc inch = 6.5” V – shaped type disc
- Producer = Robbins Ltd
- Sample holding case dimensions = 960 x 495 mm
- Electric motor = 15 (kW) (Cardu et al., 2017).

The ILCM is capable of obtaining the parameters below:

- three elements of the force applied on the disc, by triaxial load cell,
- the longidutional transposition of the test case along the cutting way with position transducer (wire type),
- the perpendicular displacement of the piston, to arrange the depth (penetration), by position transducer (wire type) (Cardu et al 2017).

### 5.2.2 Assessment Of Parameters

By means of the ILCM tests, normal force and rolling force acting on the disc cutter tool (Fig.5.10) can be easily calculated in terms of real thrust and torque required for the penetration of the disc into the rock. “ The Fn (normal force) is computed by as a function of thrust provided on each disc whereas the Fr (rolling force) is directly associated with the torque to be provided to the cutter-head to permit the rotation of the discs. The assessment of the FR allows the evaluation of the SE (specific energy) due to produced debris by the interaction between the groove so that more effective excavation can be acquired. (Cardu et al., 2017) ”.

During performing several grooves at different distances, specific energy can be optimized by knowing the most suitable ratio between spacing and penetration (s/p). After that calculation, the optimum rate for minimum SE value and optimum spacing among the tools on the cutterhead can be evaluated as well (Cardu et al. ,2017).

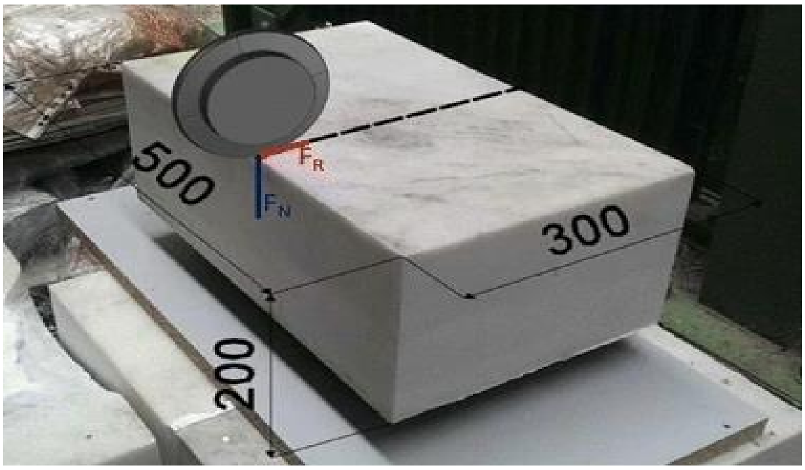


Figure 5-10:Sample used in ILCM test, Fn and Fr acting on thte disc (Cardu et al., 2017)

### 5.2.3 Data Acquisition System

The data has been obtained by using the three following steps (Montes, 2016):

- 3 channels for the triaxial load cell referred to: normal force, rolling force and side force
- 1 channel for the position of the transducer related to the longitudinal movement of the specimen case (Fig.5.11)
- 1 channel for the position of the LVDT transducer associated with the perpendicular movement of the piston (Fig.5.11)

Figure 5-11:Transducer horizontal and vertical motion (Rispoli, 2013., Montes, 2016)

By means of the transducer, measurement is made by an electronic system provided by Spider 8 software developed by HBM company. Principle of working of that system is that 8 channels can take data and perform their digitalization. Afterwards, another software which is known as Catman is used for visualisation on the screen, and finally, Microsoft Excel returns the results ( Montes, 2016).

### 5.2.4 Calibration System

The signal obtained from the triaxial load cell is changed as a unit weight in kg. After that, adequate modification has been operated to acquire values as a [kN]. The explanation is clarified by the following formulas (Montes,2016).

$$kg_{(x)} = \frac{(Volt.x - offset.x) * F.S._{(x)}}{V_{alim} * f.c\ (x) * f.a.} * 1000$$

$$kg_{(y)} = \frac{(Volt.y - offset.y) * F.S._{(y)}}{V_{alim} * f.c\ (y) * f.a.} * 1000$$

$$kg_{(z)} = \frac{(Volt.z - offset.z) * F.S._{(z)}}{V_{alim} * f.c\ (z) * f.a.} * 1000$$

where:

- kg = revert value in kg from three channels
- Volt = electrical volt value obtained
- offset = tension in volt performed on the data obtained during the calibration phase
- F.S. = triaxial load cell full scale in kg
- Valim= electrical tension which powers the cell (5 V)
- f.c. = correction element for X,Y,Z axis channel
- f.a. = amplification factor (equal to 64), (Montes,2016).

In order to confirm the position of the transducer, Rispoli (2013) has used two different signals, which are the detected signal and mechanical transducer values. The following equations show that relationship:

$$mm_{(h)} = \frac{(Volt.h - offset.h)}{V_{alim} * f.c\ (v)} * 1000$$

$$mm_{(v)} = \frac{(Volt.v - offset.v)}{V_{alim} * f.c\ (v)} * 1000$$

where:

- mm = number obtained from transducers
- Volt = electrical volt obtained
- Offset = tension in Volt implemented to the data obtained during the calibration stage
- Valim = electrical tension which powers the cell (12 V)
- f.c= corrective element; 0,48681 mV/V for longidutional transducer and 1,014 mV/V for the perpendicular one (Rispoli,2013; Montes, 2016).

### 5.2.5 Signal And Interpretation

Signal processing has been used by Rispoli (2013) to understand the detected signals without any processing and the processed signals. Furthermore, the signal has been implemented to examine the realibility of ILCM test from the signals acquired from each channel. The data were acquired when the ILCM was stopped and without contact with the rock sample.

#### 5.2.5.1 *Side force*

The not eliminated (filtered) signal is the range from +500 kg to -400 kg and after filtering that values decreased approximately 5 times, and the variation is shown in Figure 5.12. The average values are 24.4 kg and 25,6 kg incrementally (Rispoli, 2013).

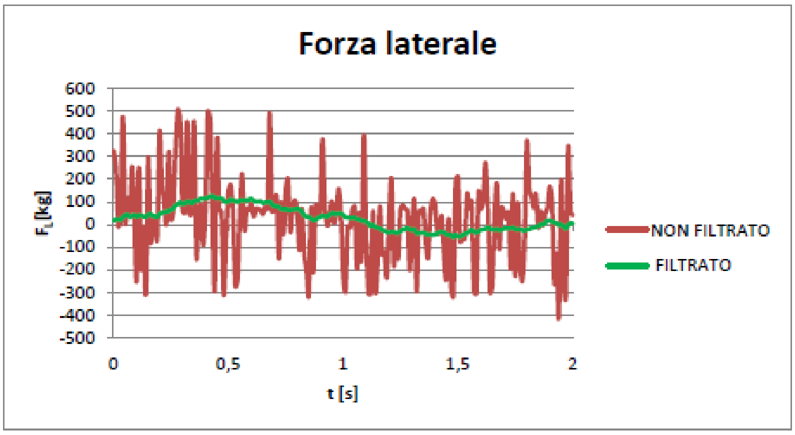


Figure 5-12:Side force comparsion (Rispoli, 2013), (Forza Laterale : lateral force. Non Filtrato : unfiltered. Filtrato : Filtered)

#### 5.2.5.2 *Rolling Force*

In this circumstance, the rolling force has a different range between +150 kg and -100 kg, whereas after the values have been filtered, the new range is +50 kg and -10 kg, seen in Figure 5.13. The average value is 20 kg and the variance is + / - 30 kg (Rispoli, 2013). According to Rispoli (2013), the rolling force has been able to provide higher values than likelihood values and from 500 kg to 1200 kg. The average value was 23,5 kg when filtered and 26,3 kg when non filtered.

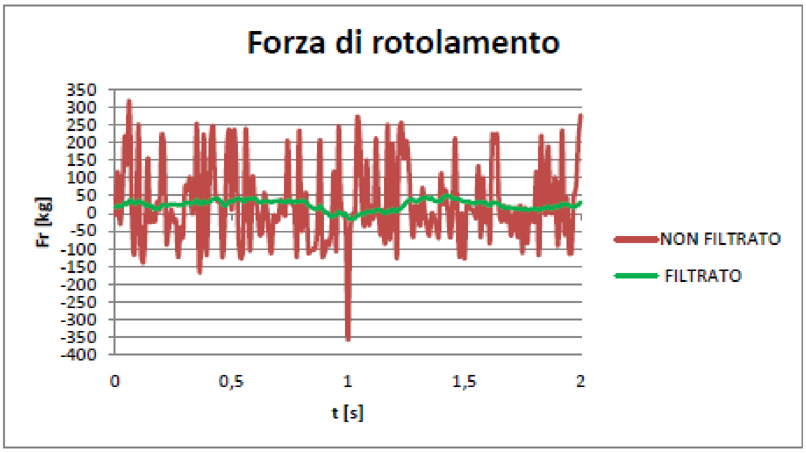


Figure 5-13:Comparison of rolling force (Rispoli, 2013), (Forza di rotolamento : rolling force. Non Filtrato : unfiltered. Filtrato : Filtered)

#### 5.2.5.3 *Normal Force*

Without filtering, the normal force (Fig.5.14) has been detected from +1000 kg to -700 kg, and after filtering the values are reduced from +100 kg to -50 kg. The average filtered Fn was 49,5 kg, whereas without filtering the value was 67,8 kg (Rispoli, 2013).

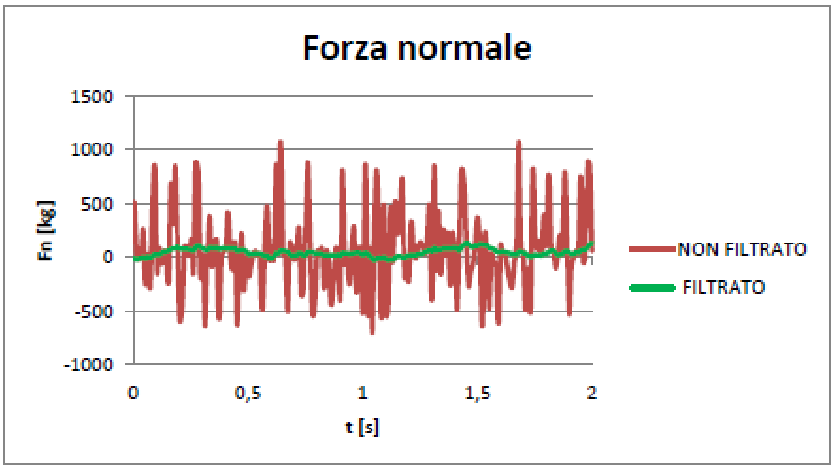


Figure 5-14:Fn comparison signals (Rispoli,2013), (Forza Normale : normal force. Non Filtrato : unfiltered. Filtrato : Filtered)

#### 5.2.5.4 *Horizontal Displacement*

The output data had a too high variance because of the filtering. Figure 5.15 shows that the variance is subordinated to 0,01 mm. The longitudinal displacement average value filtered higher than 47,12 mm (Rispoli, 2013).

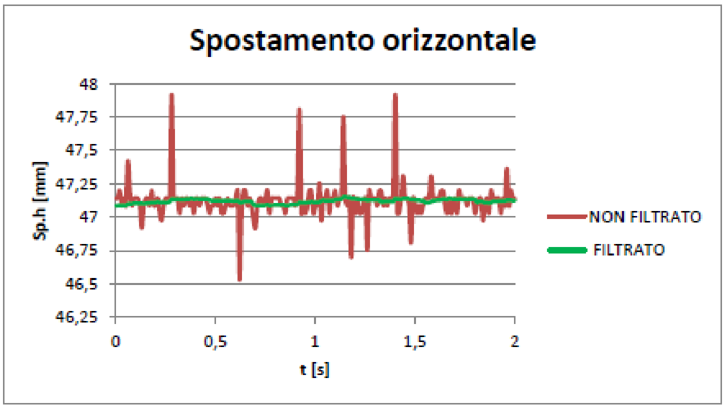


Figure 5-15:Horizontal displacement comparsion (Rispoli,2013), (Spostamento orizzontale : horizontal displacement . Non Filtrato : unfiltered. Filtrato : Filtered)

#### 5.2.5.5 *Vertical Displacement*

In this case, perpendicular displacement and its comparison are shown in Figure 5.16, and it filtered data is seen in Figure 5.17, and the measured data range was around 0,5 mm. However, the author (Rispoli, 2013) expressed that the depth of penetration has not been acceptable which were 2 mm – 4 mm. If the values are 2 mm - 4 mm, instead of average values the system has to be controlled regularly.

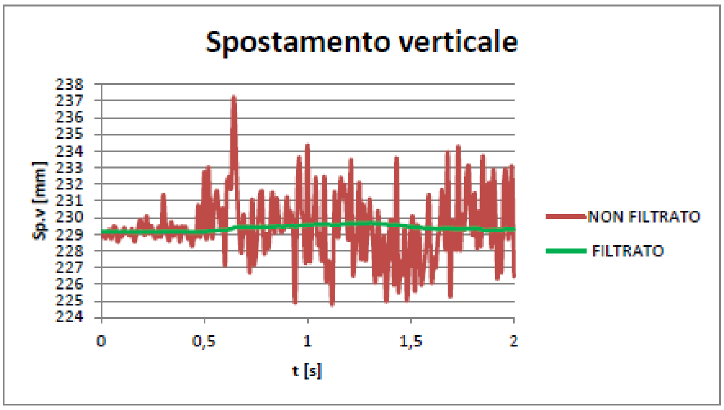


Figure 5-16:Vertical displacement comparison signals (Rispoli, 2013), (Spostamento verticale : vertical displacement . Non Filtrato : unfiltered. Filtrato : Filtered)

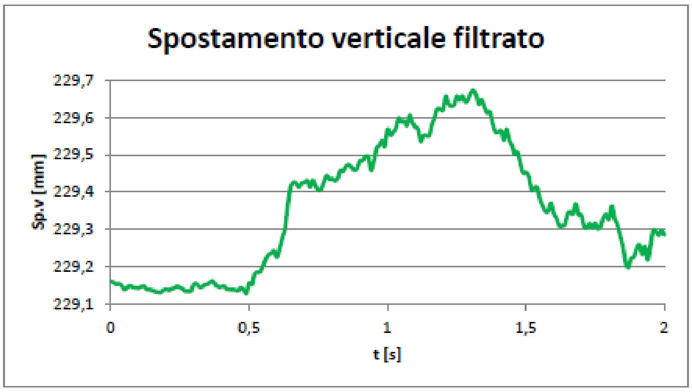


Figure 5-17:Vertical displacement filtered data (Rispoli, 2013), (Spostamento verticale filtro : vertical displacement filtered)

# 6 CHAPTER – 6

## 6.1 DICS CUTTER PERFORMANCE ANALYSIS BY USING IBM SPSS SOFTWARE THROUGH ILCM EXPERIMENTAL DATA

This chapter is the final step of the MSc Thesis. Andrea Rispoli's (2013) data, shown in Table 3, Table 4, Table 5, Table 15, Table 17 and Table 25, which have been already taken from ILCM in 2013, are here reevaluated. The data have been reanalyzed by using IBM SPSS to get a different point of view and to understand the relationship between normal force, rolling force, specific energy and cutting coefficient through more elaborative SPSS analysis methods. Generally, this type of regression analysis is made by Microsoft Excel. However, it has some restrictions, so computer-aided modelling such as IBM SPSS Statistics 25 (statistical software) has been performed to examine ILCM data and get higher level equations and regression analysis for the performance analysis of the disc cutter. The data was evaluated by Rispoli( 2013), but IBM SPSS has reevaluated the same data in terms of statistical interpretation. The purpose of IBM SPSS provides a statistical point of view, especially in terms of correlation relationship between the dependent and independent values, mean, standard deviation, p-value and Durbin Watson (autocorrelation).

## 6.2 Re – Evaluation of Rispoli (2013) data through IBM SPSS

| **"Vico" Diorite** | | | | |
|---|---|---|---|---|
| Density (kg/m$^3$) | $C_o$ (MPa) | $\sigma_{t,fle}$ (MPa) | $E_t$ (MPa) | Knopp Hardness (MPa) |
| 2620 | 124 | 21,3 | 63 | 4261 |
| **"Luserna" Stone** | | | | |
| Density (kg/m$^3$) | $C_o$ (MPa) | $\sigma_{t,fle}$ (MPa) | $E_t$ (MPa) | Knopp Hardness (MPa) |
| 2790 | 120 | 19,8 | 35 | 1286 |
| **"Prali" White Marble** | | | | |
| Density (kg/m$^3$) | $C_o$ (MPa) | $\sigma_{t,fle}$ (MPa) | $E_t$ (MPa) | Knopp Hardness (MPa) |
| 2814 | 215 | 21,1 | 45,7 | 4115 |

Table 3:Rock Sample Properties (Rispoli,2013)

### 6.2.1 Vico Diorite

The Vico Diorite data, seen in Table.4, have been acquired by Rispoli (2013) using the ILCM, and all forces have been recorded during the cutting process. Besides, during the test, the effect of non-planarity has been computed on the forces. Furthermore, the rock specimen has been put into the sample box to obtain both a positive slope (direction of cutting) and negative slope (reverse cutting movement).

The symbols of the Table.4 :

- CutN : Number of cutting,
- pmm : penetration (mm),
- smm : spacing (mm)
- s/p : spacing and penetration ratio,
- PeakFn : Peak Normal Force $(kN)$,
- PeakFr : Peak Rolling Force $(kN)$,
- CC : Cutting coefficient (%)

| CutN | pmm | smm | sp | PeakFnkN | PeakFrkN | CC |
|---|---|---|---|---|---|---|
| 1 (going) | 1,5 | - | - | 104,97 | 4,85 | 4,6 |
| 2 (return) | 1,5 | - | - | 98,87 | 7,67 | 7,8 |
| 3 (going) | 1,5 | 15 | 10 | 94,49 | 4,05 | 4,3 |
| 4 (return) | 1,5 | 15 | 10 | 87,00 | 4,73 | 5,4 |
| 5 (going) | 1,5 | 20 | 13.3 | 98,95 | 4,60 | 4,6 |
| 6 (return) | 1,5 | 20 | 13.3 | 89,86 | 5,90 | 6,6 |

Table 4:ILCM Vico Diorite Results (Rispoli, 2013) (IBM SPSS interface)

As a result, IBM SPSS analysis output that indicates peak Fn and s/p relationship, shown in Graph.1, has been acquired. The positive slope peak Fn (normal force) is higher than the negative slope.

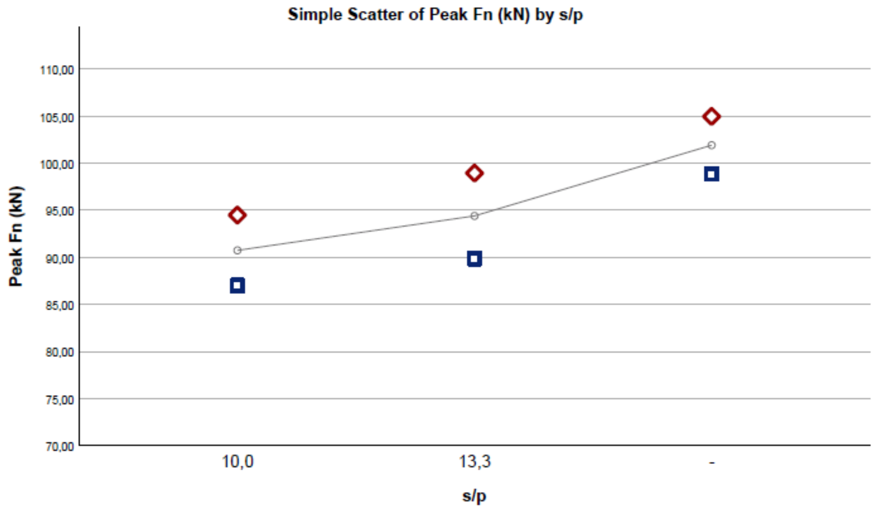


**Graph.1 :** Relationship between peak Fn And s/p by IBM SPSS, red shapes: positive slope cutting, blue shapes: negative slope cutting

Another IBM SPSS analysis output that indicates peak Fr and s/p relationship, shown in Graph.2, has been acquired. The positive slope peak Fr (normal force) is higher than the negative slope.

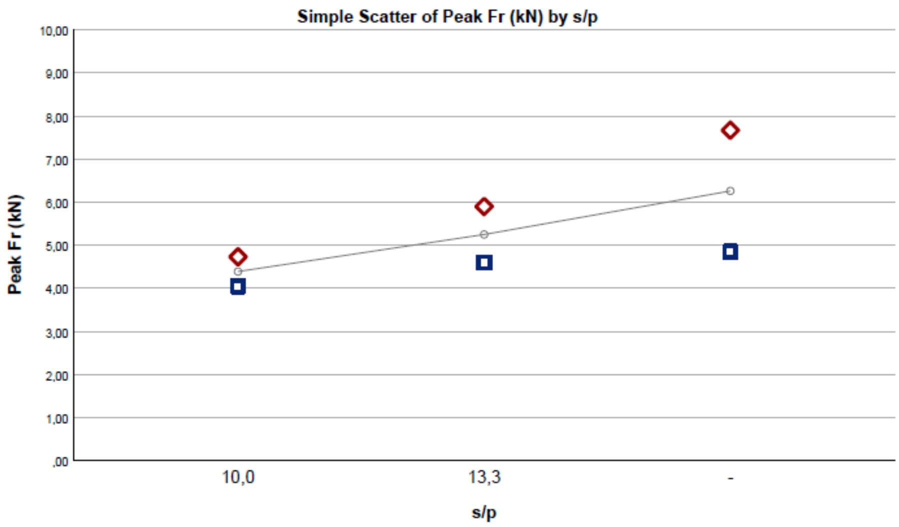


**Graph.2 :** Relationship between peak Fr And s/p by IBM SPSS, red shapes: positive slope cutting, blue shapes: negative slope cutting

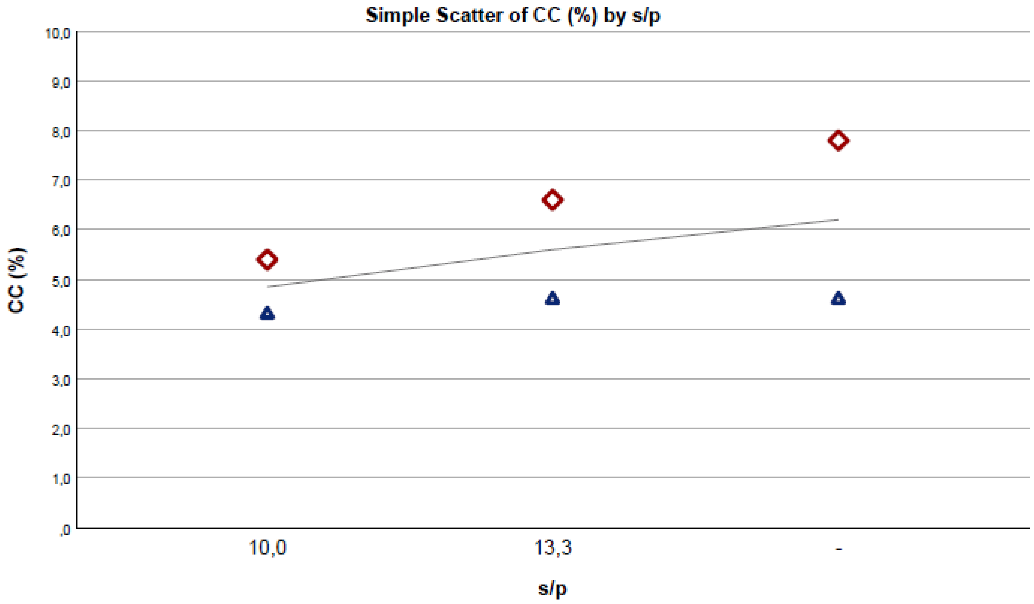


**Graph.3 :** Cutting Coefficient (CC) And s/p by IBM SPSS, red shapes : positive slope cutting, blue shapes : negative slope cutting

As it can be seen on the graphs, normal force (Graph.1), rolling force (Graph.2), and s/p have a direct proportion in both directions. However, it is clearly observed that positive slope cutting force is higher than the negative slope cutting direction in both cases. According to the results, rock specimen slope affects the CC (cutting coefficient), seen in the Graph.3, which is a function of Fr/Fn.

### 6.2.2 Luserna Stone Data Processing By IBM SPSS

| CutN | pmm | sp | MeanFnkN | PeakFnkN | MeanFrkN | Cc |
|---|---|---|---|---|---|---|
| 6 | 3,90 | 7,6 | 74,32 | 149,89 | 7,05 | 9,5 |
| 12 | 3,95 | 8,0 | 76,72 | 118,09 | 7,17 | 9,3 |
| 7 | 4,20 | 9,3 | 93,02 | 152,90 | 7,62 | 8,2 |
| 9 | 3,80 | 10,8 | 102,93 | 162,74 | 10,06 | 9,8 |
| 13 | 4,07 | 11,1 | 114,32 | 139,05 | 10,10 | 8,8 |
| 10 | 4,20 | 12,2 | 123,19 | 162,69 | 11,80 | 9,6 |

Table 5:ILCM Luserna Stone data (Rispoli, 2013)

The data have been acquired by ILCM (Rispoli, 2013), and table.5 shows the results related to Luserna Stone that were obtained during ILCM tests at Politecnico di Torino. All data have been analized by IBM SPSS software in terms of linear regression analysis.

The symbols of the Table.5 :

- CutN : Number of cutting (nominal),

- pmm : penetration (mm) (scale)
- sp : spacing and penetration ratio (scale),
- Mean Fn : Mean Normal Force ($kN$),
- Peak Fn : Peak Normal Force ($kN$),
- Mean Fr : Mean Rolling Force ($kN$),
- CC : Cutting Coefficient (%)

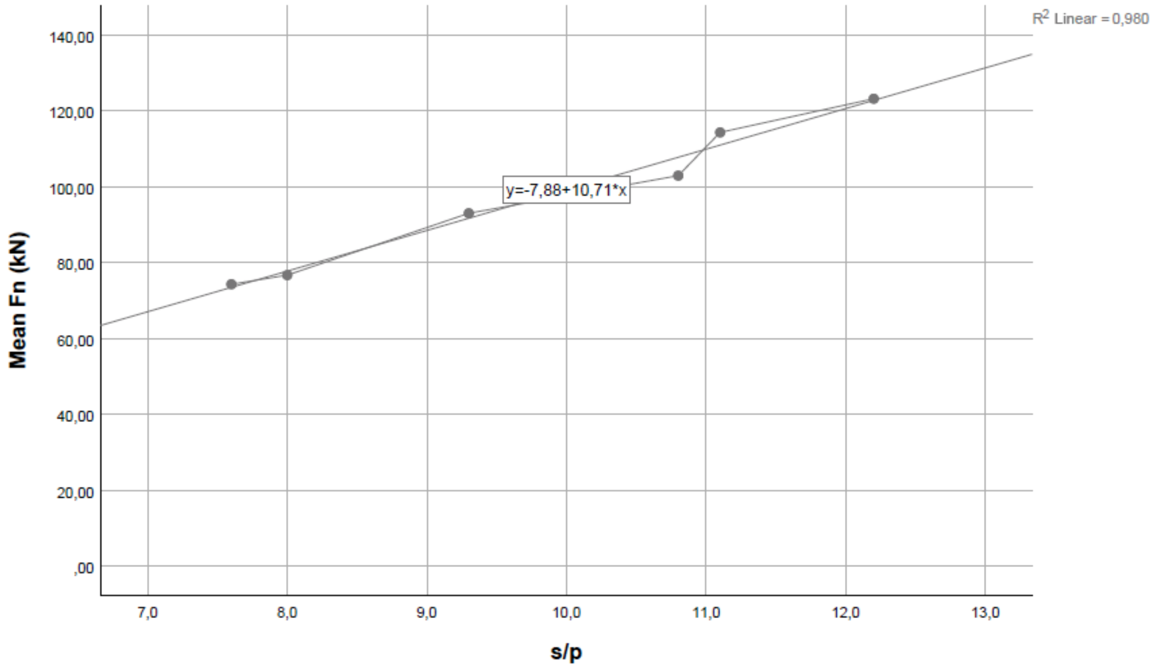


**Graph.4 :** Linear regression between mean Fn and s/p ratio

**Descriptive Statistics**

| | Mean | Std. Deviation | N |
|---|---|---|---|
| Mean Fn (kN) | 97,4167 | 19,80668 | 6 |
| s/p | 9,833 | 1,8316 | 6 |

**Correlations**

| | | Mean Fn (kN) | s/p |
|---|---|---|---|
| Pearson Correlation | Mean Fn (kN) | 1,000 | ,990 |
| | s/p | ,990 | 1,000 |
| Sig. (1-tailed) | Mean Fn (kN) | . | ,000 |
| | s/p | ,000 | . |
| N | Mean Fn (kN) | 6 | 6 |
| | s/p | 6 | 6 |

Table 6:IBM SPSS correlation and descriptive analysis

**Model Summary**[b]

| Model | R | R Square | Adjusted R Square | Std. Error of the Estimate | Durbin-Watson |
|---|---|---|---|---|---|
| 1 | ,990[a] | ,980 | ,976 | 3,09335 | 3,198 |

a. Predictors: (Constant), s/p

b. Dependent Variable: Mean Fn (kN)

Table 7:Model summary of Fn and s/p Relationship (IBM SPSS)

**Coefficients**[a]

| Model | | Unstandardized Coefficients B | Unstandardized Coefficients Std. Error | Standardized Coefficients Beta | t | Sig. |
|---|---|---|---|---|---|---|
| 1 | (Constant) | -7,879 | 7,534 | | -1,046 | ,355 |
| | s/p | 10,708 | ,755 | ,990 | 14,177 | ,000 |

**Coefficients**[a]

| Model | | 95,0% Confidence Interval for B Lower Bound | 95,0% Confidence Interval for B Upper Bound |
|---|---|---|---|
| 1 | (Constant) | -28,796 | 13,038 |
| | s/p | 8,611 | 12,805 |

a. Dependent Variable: Mean Fn (kN)

Table 8:Equation Coefficients at %95 confidence

After having examined Luserna stone data, the abovementioned outputs have been interpreted in terms of linear regression analysis, seen in Graph.4. Therefore, it is evident that there is a strong relationship between Fn (normal force) and s/p , being the regression coefficients, shown in Table 7, that is very high (99% and 98%), so it can be stated that there is a strong linear relationship among them. Furthermore, Table.6 shows that the average Fn force is 97,43 (kN), with a standard deviation of 19,80. Furthermore, the average s/p ratio is 9,83 and its standard deviation is 1,83. Besides, a linear equation can be written from the coefficients, seen in Table.8, that is given below :

$$y = -7,87 + 10,70x$$

$$Fn = -7,87 + 10,70.s/p$$

Apart from the normal force and s/p analysis, the relationship of rolling force and s/p has been analyzed by SPSS, seen in Graph.5 as well. According to outputs, it can easily be noticed that there is an excellent linear relationship between Fr and s/p that is 97,4% and 94,9%, seen in the Table.10. Furthermore, based on the Table.11 that indicates coefficients of the linear regression equation. The obtained rolling force equation is shown in below :

$$y = -1{,}28 + 1{,}043x$$

$$Fr = -1{,}28 + 1{,}043.s/p$$

Moreover, the average rolling force is 8,96 (kN) and its standard deviation is 1,96 while the mean s/p ratio is 9,83 and its standard deviation is 1,83, seen in Table.9. In addition, there is no autocorrelation between the rolling force and s/p ratio because Durbin Watson (6th column in Table.11) value is 2,09. If the Durbin Watson value is between 1,5 and 2,5, it can be stated that there is no autocorrelation among the data.

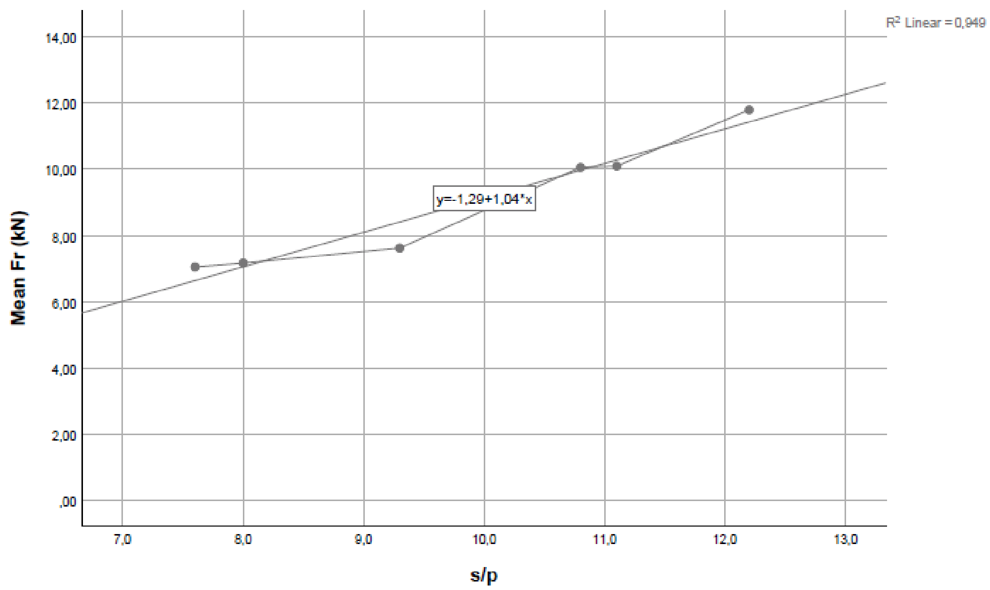


**Graph.5 :** Luserna Stone Fr and s/p linear relationship (IBM SPSS)

### Descriptive Statistics

| | Mean | Std. Deviation | N |
|---|---|---|---|
| Mean Fr (kN) | 8,9667 | 1,96075 | 6 |
| s/p | 9,833 | 1,8316 | 6 |

### Correlations

| | | Mean Fr (kN) | s/p |
|---|---|---|---|
| Pearson Correlation | Mean Fr (kN) | 1,000 | ,974 |
| | s/p | ,974 | 1,000 |
| Sig. (1-tailed) | Mean Fr (kN) | . | ,001 |
| | s/p | ,001 | . |
| N | Mean Fr (kN) | 6 | 6 |
| | s/p | 6 | 6 |

Table 9:Descriptive analysis of Luserna stone Rolling force and s/p

### Model Summary[b]

| Model | R | R Square | Adjusted R Square | Std. Error of the Estimate | Durbin-Watson |
|---|---|---|---|---|---|
| 1 | ,974[a] | ,949 | ,936 | ,49600 | 2,089 |

a. Predictors: (Constant), s/p

b. Dependent Variable: Mean Fr (kN)

Table 10:Model Summary Of Rolling Force And s/p

### Coefficients[a]

| Model | | Unstandardized Coefficients B | Unstandardized Coefficients Std. Error | Standardized Coefficients Beta | t | Sig. |
|---|---|---|---|---|---|---|
| 1 | (Constant) | -1,287 | 1,208 | | -1,066 | ,347 |
| | s/p | 1,043 | ,121 | ,974 | 8,610 | ,001 |

### Coefficients[a]

| Model | | 95,0% Confidence Interval for B Lower Bound | 95,0% Confidence Interval for B Upper Bound |
|---|---|---|---|
| 1 | (Constant) | -4,641 | 2,067 |
| | s/p | ,707 | 1,379 |

a. Dependent Variable: Mean Fr (kN)

Table 11:Luserna Stone Rolling force snd s/p ratio Linear Regression Equation

From the analysis performed, a very weak linear relationship, seen in Graph.6, is noticed between CC and s/p because R and $R^2$values, shown in Table.13, are too low (12,8% and 1,6%). However, this result could be expected due to cutting coefficient formula, that is Fr/Fn. Through that formula and results, it can be stated that the cutting coefficient is not directly related to the s/p ratio. Furthermore, the mean of cutting coefficient value is 9,2%, and the mean of s/p ratio is 9,83, seen in Table.12.

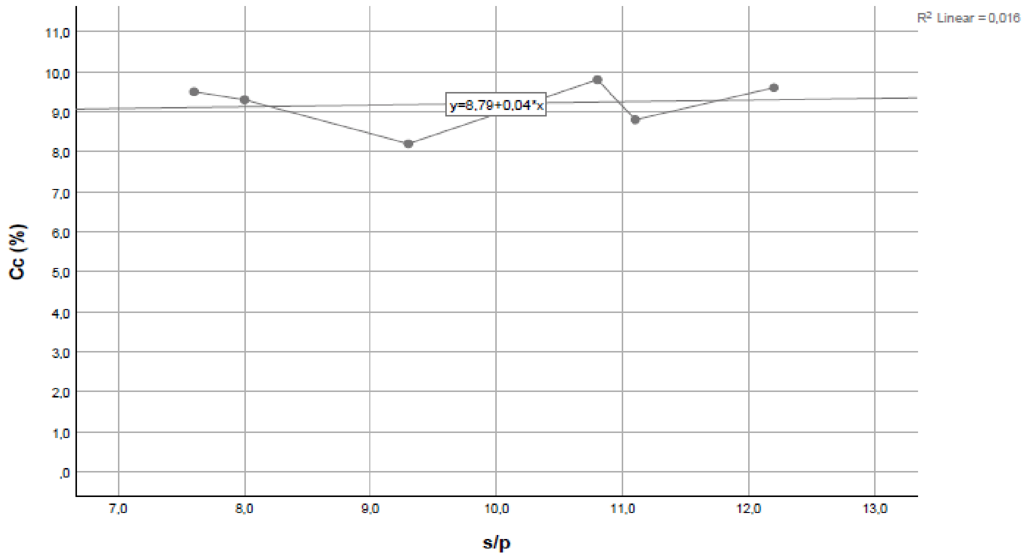


**Graph.6:** Luserna stone linear regression between CC and s/p (IBM SPSS)

**Descriptive Statistics**

| | Mean | Std. Deviation | N |
|---|---|---|---|
| Cc (%) | 9,200 | ,5967 | 6 |
| s/p | 9,833 | 1,8316 | 6 |

**Correlations**

| | | Cc (%) | s/p |
|---|---|---|---|
| Pearson Correlation | Cc (%) | 1,000 | ,128 |
| | s/p | ,128 | 1,000 |
| Sig. (1-tailed) | Cc (%) | . | ,404 |
| | s/p | ,404 | . |
| N | Cc (%) | 6 | 6 |
| | s/p | 6 | 6 |

Table 12:Luserna Stone CC and s/p Linear Regression Analysis (IBM SPSS)

**Model Summary**[b]

| Model | R | R Square | Adjusted R Square | Std. Error of the Estimate | Durbin-Watson |
|---|---|---|---|---|---|
| 1 | ,128[a] | ,016 | -,229 | ,6616 | 3,048 |

a. Predictors: (Constant), s/p

b. Dependent Variable: Cc (%)

Table 13:Output of Luserna stone linear correlation between CC and s/p

**Coefficients**[a]

| Model | | Unstandardized Coefficients B | Unstandardized Coefficients Std. Error | Standardized Coefficients Beta | t | Sig. |
|---|---|---|---|---|---|---|
| 1 | (Constant) | 8,790 | 1,611 | | 5,455 | ,005 |
| | s/p | ,042 | ,162 | ,128 | ,258 | ,809 |

**Coefficients**[a]

| Model | | 95,0% Confidence Interval for B Lower Bound | 95,0% Confidence Interval for B Upper Bound |
|---|---|---|---|
| 1 | (Constant) | 4,316 | 13,263 |
| | s/p | -,407 | ,490 |

a. Dependent Variable: Cc (%)

Table 14:Luserna Stone CC and s/p linear regression

| CutN | sp | MeanFnkN | Cutlenghtmm | Weightkg | VkN | SEMJm3 |
|---|---|---|---|---|---|---|
| 6 | 7,6 | 7,05 | 240 | ,04980 | 19,0 | 89,2 |
| 12 | 8,0 | 7,17 | 245 | ,05753 | 22,0 | 80,0 |
| 7 | 9,3 | 7,62 | 235 | ,06430 | 24,5 | 69,2 |
| 9 | 10,8 | 10,06 | 250 | ,07808 | 29,8 | 84,4 |
| 13 | 11,1 | 10,10 | 235 | ,07472 | 28,5 | 83,2 |
| 10 | 12,2 | 11,80 | 245 | ,08205 | 31,3 | 92,3 |

Table 15:Luserna stone Specific Energy from ILCM Data (Rispoli, 2013)

The meaning of the symbols on the Table.15, seen in the below :

- CutN : Number of cutting,
- s/p : spacing and penetration ratio,

- Mean Fn : Average normal force $(kN)$,
- Cut Length : Rock Sample Cutting Length (mm),
- Weight : debris weight (kg),
- V : volume of excavated debris,

  SE : Specific Energy ( MJ / $m^3$),

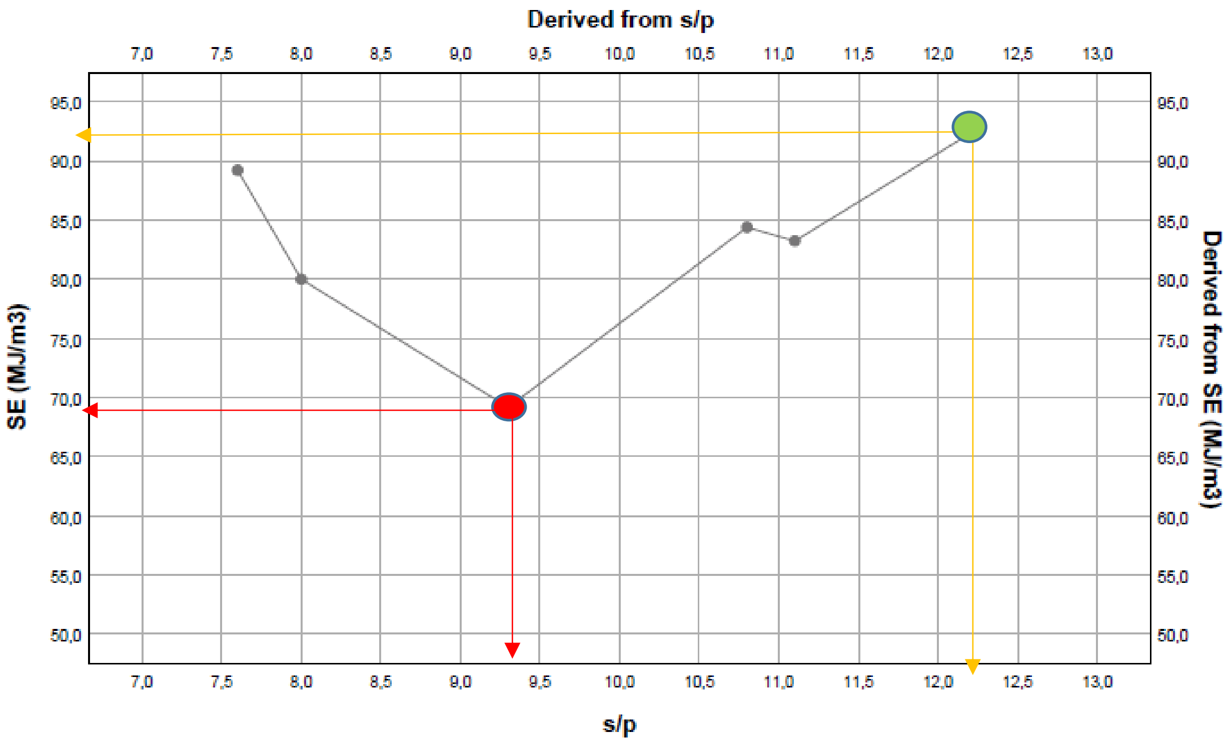


**Graph.7** : Specific Energy Vs. s/p relation obtained from Luserna stone.

The specific energy has been obtained by using the following formula:

$$SE = \frac{F_r * L_{solco}}{V}$$

where:

SE = specific energy in MJ/m$^3$

$F_r$ = rolling force in kN

$L_{solco}$ = cut length in mm

V= volume of the debris obtained from the cutting test in mm.

According to the specific energy and s/p relation, seen in graph 7, optimum s/p ratio is obtained as 9,3 (cutting number 7). It approximately corresponds to 70 (MJ/m^3) as an efficient energy consumption per meter of stone. Furthermore, it can be noticed that cutting number 10 was not efficient, as it required specific energy higher than 90 (MJ/m^3). All this analysis has been done based on the Luserna stone specific energy table, indicated in table - 15.

Apart from the previous researches (Rispoli, 2013), ILCM data relationships between the peak normal force and s/p have been examined in Luserna stone, to understand the best correlations between the rock and the tool. The linear regression of peak Fn and sp are represented in Graph.8.

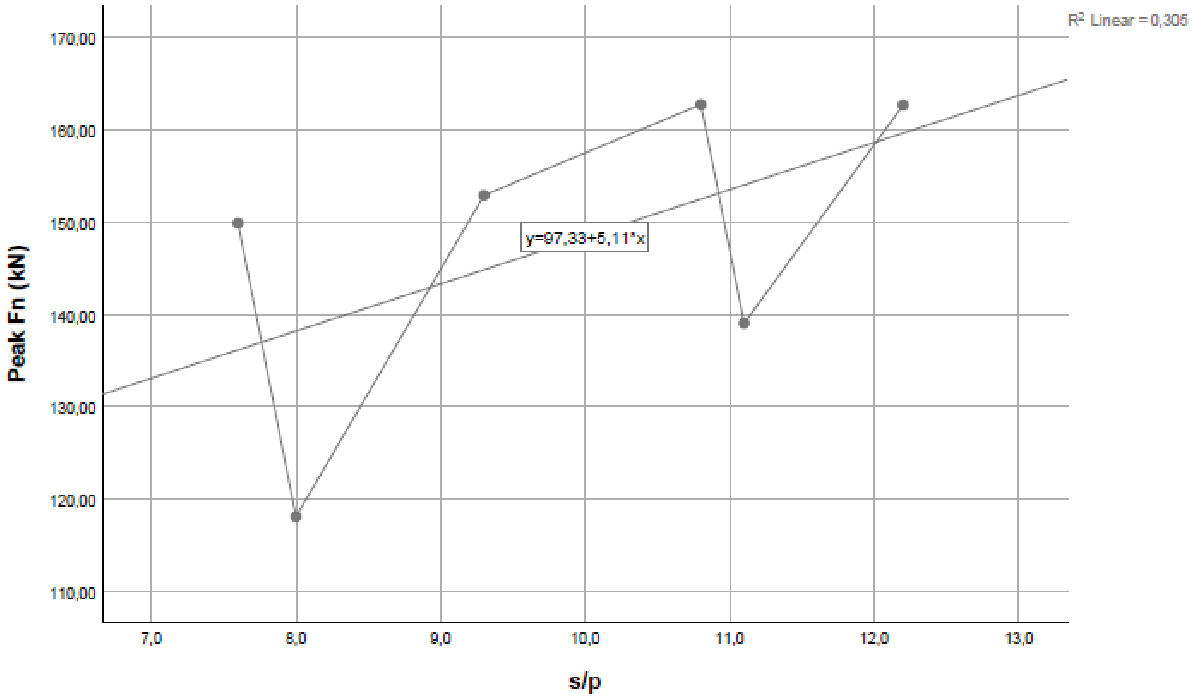


**Graph.8 :** Linear regression graph between Peak Fn and s/p ratio.

**Model Summary[b]**

| Model | R | R Square | Adjusted R Square | Std. Error of the Estimate | Durbin-Watson |
|---|---|---|---|---|---|
| 1 | ,552[a] | ,305 | ,131 | 15,78403 | 2,915 |

a. Predictors: (Constant), s/p

b. Dependent Variable: Peak Fn (kN)

Table 16:R and R square Of Peak Fn And s/p

As it can be noticed in Graph.8, there is not a strong relationship among peak Fn and s/p because R and $R^2$ values, seen in Table.16, ( 55% and 30,5% respectively) are too much lower compared to the correlation between the mean normal force and s/p (99% and 98% respectively) given in graph 4 and Table 7. Therefore, it is evident that the mean normal force is a more valid parameter than the peak normal force from ILCM tests for disc cutter performance analysis.

### 6.2.3 Prali Marble Data Processing By Using IBM SPSS

| CutN | pmm | sp | MeanFnkN | PeakFnkN | MeanFrkN | Cc |
|---|---|---|---|---|---|---|
| 8 | 3,00 | 7,3 | 58,03 | 83,40 | 4,77 | 8,2 |
| 2 | 2,85 | 9,0 | 70,74 | 86,86 | 5,08 | 7,2 |
| 4 | 2,85 | 11,0 | 71,62 | 104,32 | 6,92 | 9,7 |
| 5 | 2,80 | 11,9 | 75,71 | 99,00 | 7,95 | 10,5 |
| 6 | 2,85 | 13,5 | 83,02 | 104,33 | 8,16 | 9,8 |
| 9 | 2,95 | 15,3 | 94,60 | 102,63 | 8,86 | 9,4 |
| 10 | 2,95 | 16,2 | 102,99 | 112,50 | 9,39 | 9,1 |
| 11 | 2,95 | 16,9 | 106,76 | 110,60 | 9,71 | 9,1 |
| 12 | 2,90 | 17,5 | 108,95 | 111,70 | 9,89 | 9,1 |

Table 17:ILCM Prali Marble Data (A. Rispoli, 2013)

- CutN : Number of cutting (nominal),
- pmm : penetration (mm) (scale)
- sp : spacing and penetration ratio (scale),
- Mean Fn : Mean Normal Force $(kN)$,
- Peak Fn : Peak Normal Force $(kN)$,
- Mean Fr : Mean Rolling Force $(kN)$,
- CC : Cutting Coefficient (%)

The data from Prali Marble, seen in Table.17, have been recorded by Rispoli (2013) using ILCM. Also in this case, the data will be examined by IBM SPSS in terms of linear regression analysis, to understand the strong and weak linear relationships between them, with the aim to evaluate the disc cutter performance. The results of the analyses are given in the following pages. Data from Prali Marble are provided in Table.17. In terms of linear regression analysis, the normal force, rolling force, cutting coefficient, specific energy and normal peak force/s/p relationships are considered.

There is a strong linear relation, shown in Graph.9, between mean normal force and s/p based on R and $R^2$ values, seen in Table.19, (98% and 96,4% respectively). Moreover, the average normal force is 85,82 (kN) , and its standard deviation is 18,22, are indicated in Table.18. Otherwise, mean of s/p value is 13,17 and its standard deviation is 3,61, are represented in Table.19. Furthermore, the slope equation has been acquired from the coefficients in Table 21. The following formula shows the slope equation for Prali Marble:

y = 20,95 + 4,95x    Fn = 20,95 + 4,95.s/p

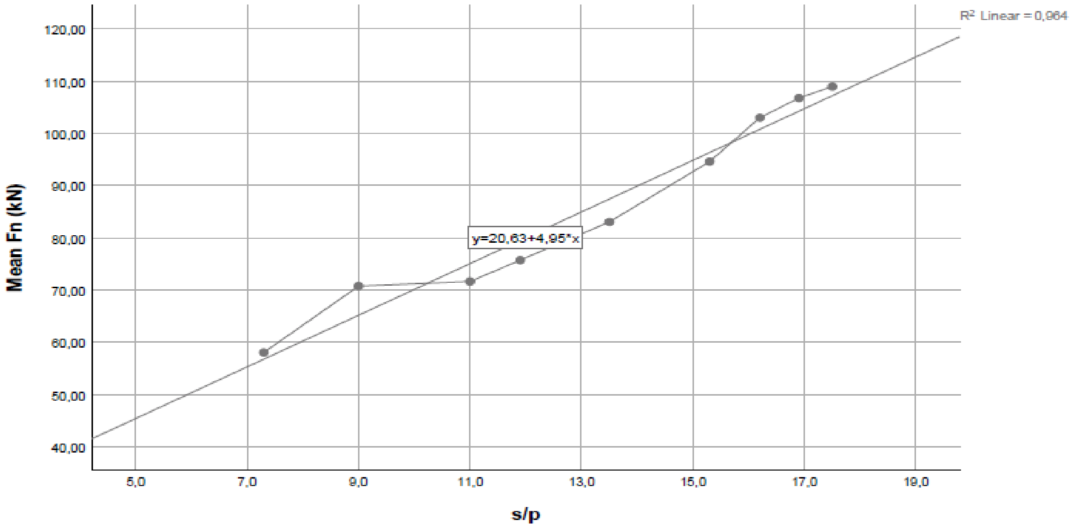


**Graph.9 :** Prali Marble FN and s/p ratio linear relation

## Descriptive Statistics

| | Mean | Std. Deviation | N |
|---|---|---|---|
| Mean Fn (kN) | 85,8244 | 18,22347 | 9 |
| s/p | 13,178 | 3,6169 | 9 |

Table 18:Prali Marble Average Normal Force And Mean Of s/p

## Model Summary[b]

| Model | R | R Square | Adjusted R Square | Std. Error of the Estimate | Durbin-Watson |
|---|---|---|---|---|---|
| 1 | ,982[a] | ,964 | ,959 | 3,69547 | 1,293 |

a. Predictors: (Constant), s/p

b. Dependent Variable: Mean Fn (kN)

Table 19:Assesment of the orrelation between FN and s/p (Prali marble).

**Coefficients[a]**

| Model | | Unstandardized Coefficients B | Unstandardized Coefficients Std. Error | Standardized Coefficients Beta | t | Sig. |
|---|---|---|---|---|---|---|
| 1 | (Constant) | 20,635 | 4,917 | | 4,197 | ,004 |
| | s/p | 4,947 | ,361 | ,982 | 13,695 | ,000 |

**Coefficients[a]**

| Model | | 95,0% Confidence Interval for B Lower Bound | 95,0% Confidence Interval for B Upper Bound |
|---|---|---|---|
| 1 | (Constant) | 9,008 | 32,262 |
| | s/p | 4,093 | 5,801 |

a. Dependent Variable: Mean Fn (kN)

Table 20:FN and s/p slope equation coefficients at %95 confidence (Prali marble)

According to SPSS outputs, the rolling force and s/p have a strong linear correlation depending on the results provided in Table.22, in terms of R and $R^2$ coefficients (98 %and 96,4% respectively); also, the average rolling force is 7,85 (kN) and the rolling force standard deviation is 1,9, expressed in Table.21. The average s/p is 13.17, and its standard deviation is 3.61, shown in Table.21. In addition, there is no autocorrelation between the rolling force and s/p, because the Durbin Watson value is 1,65 (so, between 1,5 and 2,5). Using the coefficients provided in Table.23, the slope equation can been expressed for rolling force as follows:

$$y = 1,03 + 0,52x$$

$$Fr = 1,03 + 0,52.s/p \ ( R^2 = \%96)$$

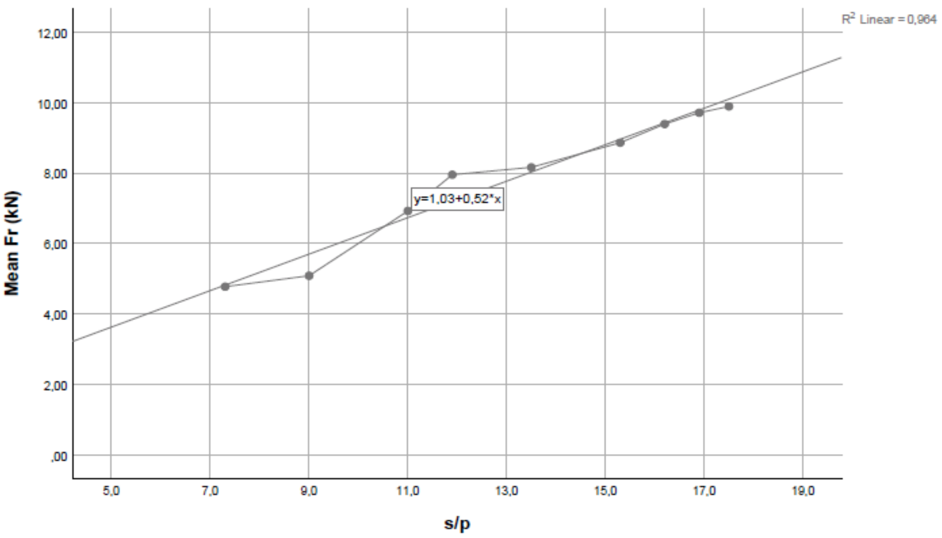


**Graph.10 :** Prali Marble linear correlation between Rolling force and s/p

## Descriptive Statistics

| | Mean | Std. Deviation | N |
|---|---|---|---|
| Mean Fr (kN) | 7,8589 | 1,90861 | 9 |
| s/p | 13,178 | 3,6169 | 9 |

Table 21:Mean values of Rolling Force and s/p (Prali marble).

## Model Summary[b]

| Model | R | R Square | Adjusted R Square | Std. Error of the Estimate | Durbin-Watson |
|---|---|---|---|---|---|
| 1 | ,982[a] | ,964 | ,958 | ,38926 | 1,650 |

a. Predictors: (Constant), s/p

b. Dependent Variable: Mean Fr (kN)

Table 22:Rolling force and s/p linear correlation (Prali marble)

## Coefficients[a]

| Model | | Unstandardized Coefficients B | Unstandardized Coefficients Std. Error | Standardized Coefficients Beta | t | Sig. |
|---|---|---|---|---|---|---|
| 1 | (Constant) | 1,033 | ,518 | | 1,994 | ,086 |
| | s/p | ,518 | ,038 | ,982 | 13,613 | ,000 |

## Coefficients[a]

| Model | | 95,0% Confidence Interval for B Lower Bound | 95,0% Confidence Interval for B Upper Bound |
|---|---|---|---|
| 1 | (Constant) | -,192 | 2,258 |
| | s/p | ,428 | ,608 |

a. Dependent Variable: Mean Fr (kN)

Table 23:Slope trendline coefficients Fr and s/p (Prali Marble)

As it can be seen from Graph.11 and Table.24, the cutting coefficient and s/p have not strong linear correlation due to very low percentages of R and $R^2$ square (39,7% and 15,8% respectively). Especially $R^2$is too low because the cutting coefficient does not directly depend on s/p. The CC is derived from the ratio between rolling force and normal force.

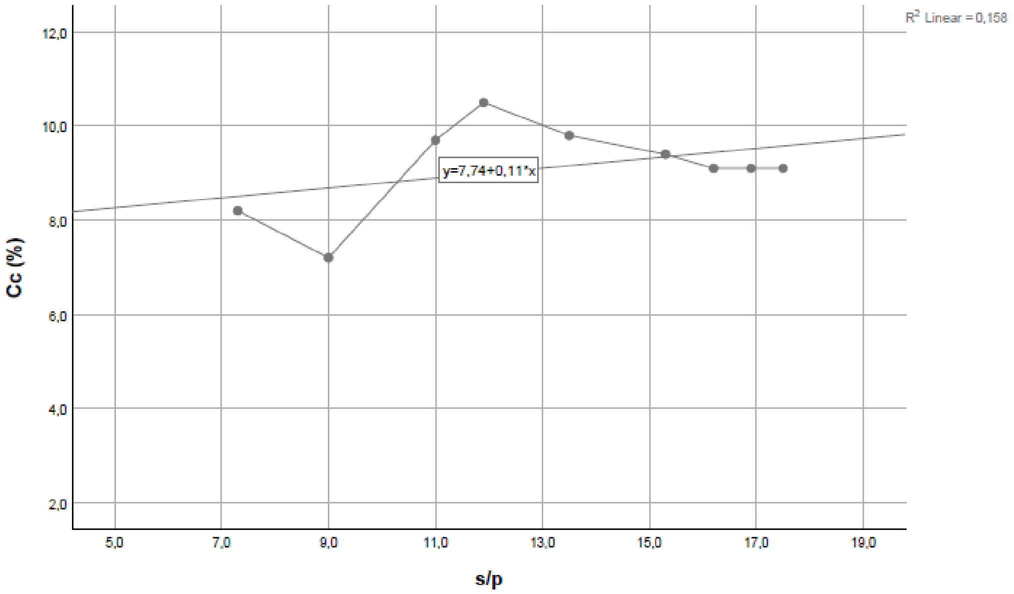


**Graph.11 :** Prali Marble CC ands/p Linear Relation

**Model Summary**[b]

| Model | R | R Square | Adjusted R Square | Std. Error of the Estimate | Durbin-Watson |
|---|---|---|---|---|---|
| 1 | ,397[a] | ,158 | ,038 | ,9381 | 1,363 |

a. Predictors: (Constant), s/p

b. Dependent Variable: Cc (%)

Table 24:CC and s/p Correlation Summary

| CutN | sp | MeanFnkN | Cutlenghtmm | Weightkg | VkN | SEMJm3 |
|---|---|---|---|---|---|---|
| 8 | 7,3 | 4,77 | 205 | ,06205 | 22,2 | 43,97 |
| 2 | 9,0 | 5,08 | 210 | ,07161 | 25,7 | 41,57 |
| 4 | 11,0 | 6,92 | 200 | ,09616 | 34,5 | 40,16 |
| 5 | 11,9 | 7,95 | 210 | ,11936 | 42,8 | 39,03 |
| 6 | 13,5 | 8,16 | 225 | ,15482 | 55,5 | 33,08 |
| 9 | 15,3 | 8,86 | 210 | ,20999 | 75,3 | 24,72 |
| 10 | 16,2 | 9,39 | 215 | ,20918 | 75,0 | 26,93 |
| 11 | 16,9 | 9,71 | 220 | ,19823 | 71,1 | 30,07 |
| 12 | 17,5 | 9,89 | 220 | ,19365 | 69,4 | 31,35 |

Table 25:Prali Marble Specific Energy And s/p ratio ILCM (A. Rispoli, 2013)

- CutN : Number of cutting,
- s/p : spacing and penetration ratio,
- Mean Fn : Average normal force $(kN)$,
- Cut Length : Rock Sample Cutting Length (mm),
- Weight : debris weight (kg),
- V : volume of excavated debris,
- SE : Specific Energy ( MJ / $m^3$),

According to Table.25 and Graph.12, optimum s/p ratio is 15,3 and it corresponds to an energy consumption of about 24,72 (MJ/$m^3$) in cutting number 9 whereas the most inefficient s/p ratio is 7,3 and it refers to very high energy consumption 43,97 (MJ/$m^3$).

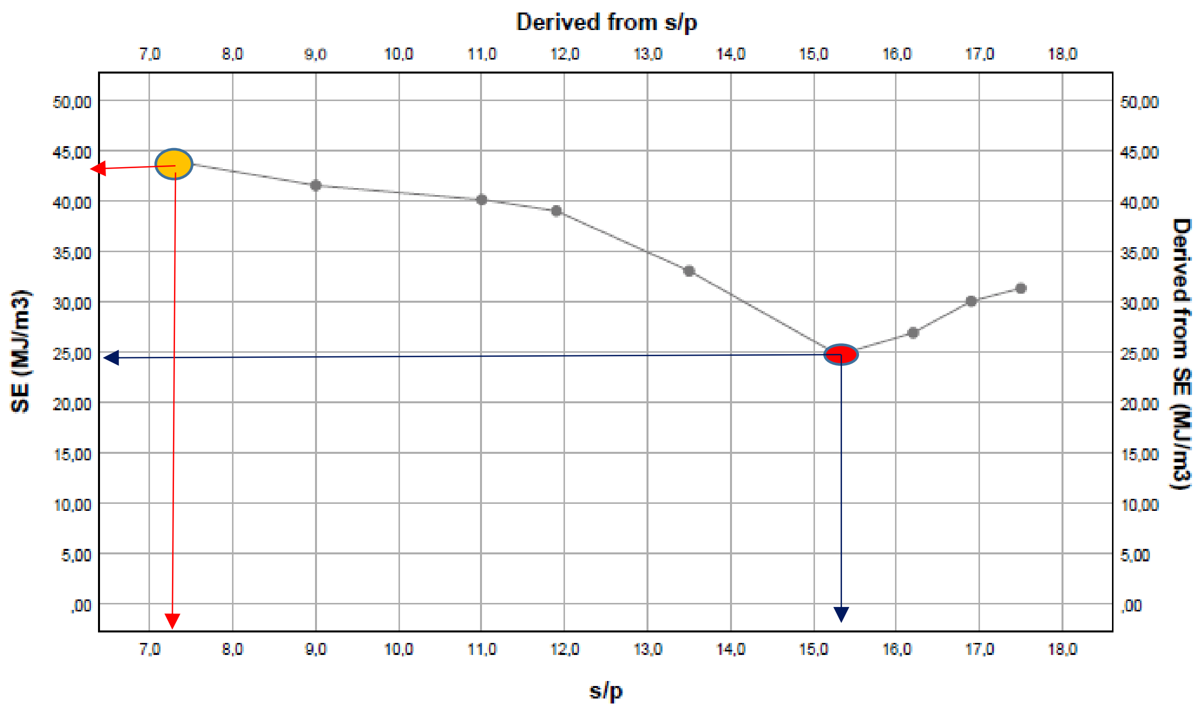


**Graph.12 :** Trend of the Specific Energy Vs. s/p ratio (Prali marble).

The Prali marble has a high linear correlation between peak normal force and s/p ratio. It can be easily noticed from table.27 that R and $R^2$ values are 92,3% and 85,3%. However, there is no autocorrelation between peak Fn and s/p because the Durbin Watson, seen in Table.27, the value is 2,5, (so, between 1,5 and 2,5). Moreover, the average peak normal force value is 101.7 $(kN)$ and the average s/p value is 13.17, shown in Table.26. Besides, the slope equation is derived from Graph.13, as reported below :

$$y = 66,56 + 2,62x \quad \text{Peak Fn} = 66,56 + 2,62.s/p$$

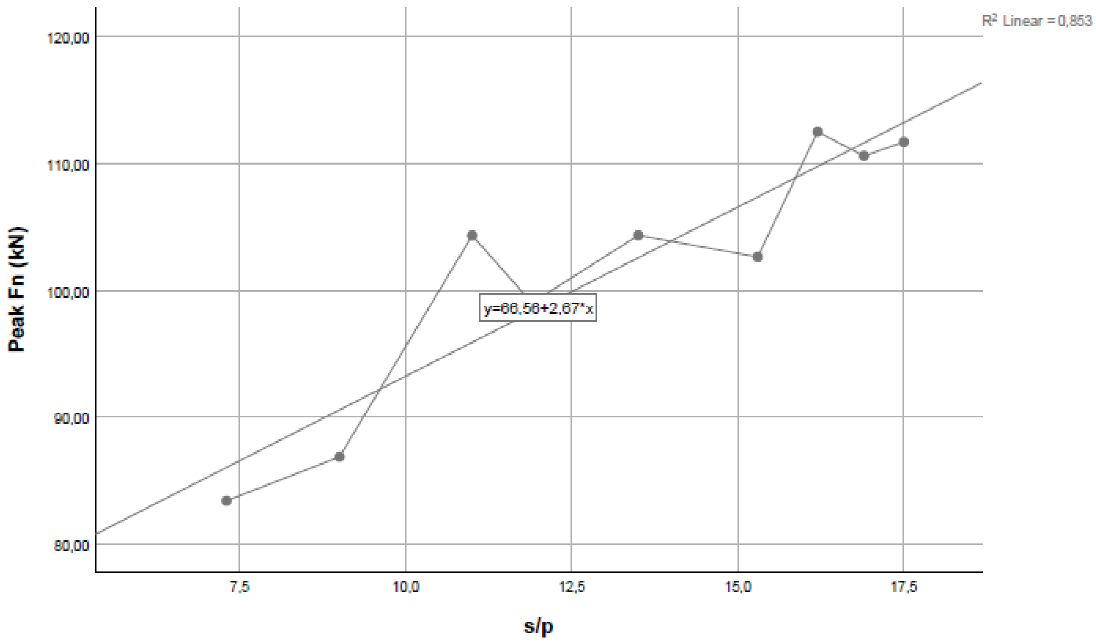


**Graph.13 :** Peak FN Vs s/p linear trend (Prali marble).

### Descriptive Statistics

| | Mean | Std. Deviation | N |
|---|---|---|---|
| Peak Fn (kN) | 101,7044 | 10,44570 | 9 |
| s/p | 13,178 | 3,6169 | 9 |

Table 26:Mean And Standard Deviation of Peak FN and s/p

### Model Summary[b]

| Model | R | R Square | Adjusted R Square | Std. Error of the Estimate | Durbin-Watson |
|---|---|---|---|---|---|
| 1 | ,923[a] | ,853 | ,832 | 4,28445 | 2,501 |

a. Predictors: (Constant), s/p

b. Dependent Variable: Peak Fn (kN)

Table 27:Linear Correlation Between Peak FN and s/p

## 6.3 Comparison among data processing output values coming from Prali, Luserna and Vico diorite samples

The IBM SPSS 25 software has been employed for the abovementioned rock specimens in terms of linear regression analysis, to elaborate outputs. Initially, the Vico diorite were not analyzed in terms of linear regression due to unrecorded mean normal force. However, it has been examined in terms of inclination of sample and sample box, and it has been noticed that it required higher normal force in a positive direction than in negative direction cutting, as in Graph.1. Furthermore, there is a direct proportion between FN peak and s/p in that rock sample. In addition, the direct proportion is prevailing for rolling force and s/p ratio.

Unlike the Vico diorite, the linear regression analysis has been provided both for Luserna stone and Prali marble in order to understand the ILCM disc cutter performance in two different rock specimens. First, the Luserna stone has a strong linear correlation between mean normal force and s/p ratio, as it can be seen in Table.7 and Graph.4, whereas there is a quite low linear correlation between Fn peak force and s/p in the Luserna stone, as reported in Table.16 and Graph.8. Furthermore, due to the mechanical properties of rock samples, the Luserna stone has required a higher normal force and a higher peak normal force (Table.5) than the Prali marble (Table.17). Moreover, the average s/p ratio of Luserna stone (Graph.7) is lower than that of Prali marble (Graph.12). Both Prali marble and Luserna stone have highly significant level linear relation in terms of rolling force, and s/p ratio, and the values are given in Table.10 and Table.22. The standard deviation of rolling force and normal force of the Luserna stone are 19,6 and 1,96 respectively. The standard deviation of the rolling force and normal force of the Prali marble are 18,22 and 1,90. The standard deviation of the Luserna stone is slightly higher than the standard deviation of the Prali Marble. The linear regression analysis of the cutting coefficients of both stones are not satisfying due to too weak R and $R^2$ correlation in both cases (Table 15 and Table 24).

A prominent output of the IBM SPSS is related to a linear correlation between peak normal force and s/p ratio of the Prali marble: in fact, unlike the Luserna stone, it exhibits a perfect linear regression between FN peak and s/p (Table 27).

In terms of specific energy related to Prali marble and Luserna stone, it can be noticed that the mechanical excavation requires 24,72 MJ/$m^3$ Prali marble; in contrast, the same machine needs more energy consumption in Luserna stone, 70 MJ/$m^3$. In terms of energy requirements, the optimum s/p ratio in Luserna stone is lower than that of Prali marble to acquire good penetration into the samples.

# 7 CONCLUSION

In this study, the TBM (tunnel boring machine) and its cutter tools have been examined by using many references. Initially, the history of the mechanized tunnelling has been mentioned with different historical examples. After that, the different sort of the TBM and the areas of their operations have been discussed. Furthermore, the literature of the TBM performance in the hard rock has been analyzed by utilizing previous work of the hard rock condition models.

Moreover, the selection criteria of the TBM has been presented by geology, site information, orientation and capital cost.

Apart from the TBM and its properties, the master thesis has mentioned rock cutting tools (chisel tools and disc cutter tools), and the rock cutting theories have been analyzed. In addition, the performance analysis of the disc cutters has been examined by employing different previous scientific works.

In chapter four, except for empirical and theoretical performance analysis models, application of computer-aided modelling methods (machine learning and statistical models) for TBM and cutter tools performance analysis have been mentioned.

After chapter four, one of the experimental methods that are called LCM (Linear Cutting Machine) has been explained. The components of the machine, rock mass tool interaction of the machine and interpretation of the outputs have been expressed.

In chapter five, another experimental method that is known as ILCM (intermediate linear cutting machine) has been presented. The components, applicability, dimensions and required size rock sample of the ILCM is explained.

At the end of the thesis, Italian stones which are Vico Diorite, Luserna Stone and Prali Marble have been analyzed by IBM SPSS computer-aided method. The interpreted data has been obtained from the ILCM. Linear regression methods have examined the collected data, and each force (normal force and rolling force) have been plotted in spacing/penetration ratio. Each output has been explained in terms of R and R square (dependent and independent correlation), mean force and average s/p ratio (descriptive analysis).

In consequence, each rock sample provided a good correlation between force and s/p ratio, whereas they provided a weak correlation between cutting coefficient and s/p ratio. Moreover, it can easily be seen that computer-aided modelling methods present more elaborative results in terms of data analysis of the output.

In future work, to obtain more reliable and understandable results between cutter tools and rock sample interaction computer-aided methods will take critical role not only in industry and but also in laboratory works. Besides, the computer-aided models (machine learning, deep learning, statistical models and artificial intelligence), are competent methods to eliminate errors and also works in a high amount of the data.

# 8 REFERENCES


Alireza Salimi, Jamal Rostami, Christian Moormann, and Andrea Delisio.Application of non-linear regression analysis and artificial intelligence al-gorithms for performance prediction of hard rock tbms.Tunnelling andUnderground Space Technology, 58:236–246, 2016

Amund Bruland.Hard rock tunnel boring. Fakultet for ingeniørvitenskapog teknologi, 2000

Bernhard Maidl, Leonhard Schmid, Willy Ritz, and Martin Herrenknecht.Hardrock tunnel boring machines. John Wiley & Sons, 2008.

Bernhard Maidl, Markus Thewes, and Ulrich Maidl.Handbook of Tunnel Engineering I: Structures and Methods, volume 1. John Wiley & Sons,2013.

Bernhard Maidl, Martin Herrenknecht, Ulrich Maidl, and Gerhard Wehrmeyer. Mechanised shield tunnelling. John Wiley & Sons, 2013.

Bjorn Nilsen, Levent Özdemir. Hard Rock Tunnel Boring Prediction And Field Performance, Chapter 52, 1993, NTNU, CSM – EMI

C Balci and N Bilgin. Correlative study of linear small and full-scale rockcutting tests to select mechanized excavation machines.International jour-nal of rock mechanics and mining sciences (1997), 44(3):468–476, 2007

C Balci. Correlation of rock cutting tests with field performance of a tbm ina highly fractured rock formation: a case study in kozyatagi-kadikoy metrotunnel, turkey.Tunnelling and Underground Space Technology, 24(4):423–435, 2009.

Chang, S.-H., Choi, S.-W., Bae, G.-J. & Jeon, S., 2006. Performance prediction of TBM disc cutting on granitic rock by linear cutting disc. Tunneling and Underground Space Technology , Issue 21.

Choice of TBM type for mountain tunnelling under very poor geological conditions: Hybrid, Slurry, Epb, Dsu, Convertible Tbms, WTC 2018, Remo Grandori1 , Antonio De Biase 2 , Marco D'Ambrosio, Seli Overseas S.p.A

David N Chapman, Nicole Metje, and Alfred Stark.Introduction to tunnel construction. Crc Press, 2017.

DF Howarth et al. The effect of jointed and fissured rock on the per-formance of tunnel boring machines. InISRM International Symposium.International Society for Rock Mechanics and Rock Engineering, 1981

F Dahl. Dri, bwi, cli standards. NTNU, Angleggsdrift, Trondheim, 20 ,2003.

Frank F Roxborough and Huw R Phillips. Rock excavation by disc cut-ter. InInternational Journal of Rock Mechanics and Mining Sciences &Geomechanics Abstracts, volume 12, pages 361–366. Elsevier, 1975

G Barla. Tbm tunneling in deep underground excavation in hard rock withspalling behaviour. In Proceedings of the 43rd Geomechanics Colloquium,pages 25–39, 2014

Hai Xu, Jian Zhou, Panagiotis G Asteris, Danial Jahed Armaghani, and Mahmood Md Tahir.Supervised machine learning techniques to theprediction of tunnel boring machine penetration rate.Applied Sciences,9 (18): 3715, 2019.

Hans U Aeberli, AEBERLI HU, et al. On the influence of discontinuitiesat the application of tunnelling machines. 1978

Hayati Yenice, Mehmet V ̇Ozdo ̆gan, and M Kemal ̇Ozfırat. A sampling study on rock properties affecting drilling rate index (dri). Journal ofAfrican Earth Sciences, 141:1–8, 2018.

Hongsu Ma, Qiuming Gong, Ju Wang, Lijun Yin, and Xiaobao Zhao. Study on the influence of confining stress on tbm performance in granite rock bylinear cutting test.Tunnelling and Underground Space Technology, 57:145–150, 2016

J Rostami, R Gertsch, and L Gertsch. Rock fragmentation by disc cutter:a critical review and an update. In Proceedings of North American rockmechanics symposium (NARMS’02), Toronto, Ontario, 2002

Jafar Hassanpour, Jamal Rostami, and Jian Zhao. A new hard rock tbmperformance prediction model for project planning.Tunnelling and Under-ground Space Technology, 26(5):595–603, 2011.

Jamal Rostami. Performance prediction of hard rock tunnel boring ma-chines (tbms) in difficult ground.Tunnelling and Underground Space Tech-nology, 57:173–182, 2016.

Jamal Rostami, Levent Ozdemir, and Bjorn Nilson. Comparison between csm and nth hard rock tbm performance prediction models. In Proceedingsof Annual Technical Meeting of the Institute of Shaft Drilling Technology,Las Vegas, pages 1–10, 1996.

Jamal Rostami. Study of pressure distribution within the crushed zone inthe contact area between rock and disc cutters.International Journal ofRock Mechanics and Mining Sciences, 57:172–186, 2013

Joakim Navestad Hansen. Comparison of existing performance predictionmodels for hard rock tunnel boring based on data collected at the follo lineproject. Master’s thesis, NTNU, 2018.

Joe Roby, Tyler Sandell, John Kocab, and Leif Lindbergh. The currentstate of disc cutter design and development directions. In Proceedings of 2008 North American Tunnelling Conference (NAT2008), Society for Min-ing, Metallurgy & Exploration, pages 36–45, 2008

Jung-Woo Cho, Seokwon Jeon, Ho-Young Jeong, and Soo-Ho Chang. Evaluation of cutting efficiency during tbm disc cutter excavation within a ko-rean granitic rock using linear-cutting-machine testing and photogrammet-ric measurement.Tunnelling and Underground Space Technology, 35:37–54,2013

Kaushik Dey and AK Ghose. Review of cuttability indices and a new rock-mass classification approach for selection of surface miners.Rock mechanicsand rock engineering, 44(5):601, 2011.

L Ozdemir. Csm computer model for tbm performance prediction.ColoradoSchool of Mines, 2003

Laikuang Lin, Yimin Xia, and Dun Wu. Multiobjective optimization de-sign for structural parameters of tbm disc cutter rings based on fahp andsampga.Advances in Civil Engineering, 2019, 2019.

Lihui Wang, Yilan Kang, Xiangjun Zhao, and Qian Zhang. Disc cutterwear prediction for a hard rock tbm cutterhead based on energy analysis.Tunnelling and Underground Space Technology, 50:324–333, 2015.

M Alvarez Grima, PA Bruines, and PNW Verhoef. Modeling tunnel boringmachine performance by neuro-fuzzy methods. Tunnelling and underground space technology, 15(3):259–269, 2000

M Sapigni, M Berti, E Bethaz, A Busillo, and G Cardone. Tbm perfor-mance estimation using rock mass classifications.International Journal of Rock Mechanics and Mining Sciences, 39(6):771–788, 2002

Marilena Cardu, Giorgio Iabichino, Pierpaolo Oreste, and Andrea Rispoli.Experimental and analytical studies of the parameters influencing the ac-tion of tbm disc tools in tunnelling.Acta Geotechnica, 12(2):293–304, 2017.

Martin Entacher and Jamal Rostami. Tbm performance prediction modelwith a linear base function and adjustment factors obtained from rock cut-ting and indentation tests.Tunnelling and Underground Space Technology,93:103085, 2019

Martin Herrenknecht and Ulrich Rehm. Mixshield technology. In Proceeding of Soft Ground and Hard Rock Mechanical Tunneling Technology Seminar,Colorado-USA, 2003, 2003

MC Villeneuve. Hard rock tunnel boring machine penetration test as anindicator of chipping process efficiency.Journal of Rock Mechanics and Geotechnical Engineering, 9(4):611–622, 2017

Navid Afrasiabi, Ramin Rafiee, and Mehdi Noroozi. Investigating the effect of discontinuity geometrical parameters on the tbm performance in hardrock.Tunnelling and Underground Space Technology, 84:326–333, 2019.

Nuh Bilgin, Hanifi Copur, and Cemal Balci.Mechanical excavation inmining and civil industries. CRC press, 2013.

Nuh Bilgin, Hanifi Copur, and Cemal Balci. Effect of replacing disc cutterswith chisel tools on performance of a tbm in difficult ground conditions.Tunnelling and Underground Space Technology, 27(1):41–51, 2012.

Nuh Bilgin, Hanifi Copur, and Cemal Balci.TBM excavation in difficultground conditions: case studies from Turkey. John Wiley & Sons, 2016.

R Gertsch, L Gertsch, and Jamal Rostami. Disc cutting tests in coloradored granite: Implications for tbm performance prediction.InternationalJournal of rock mechanics and mining sciences, 44(2):238–246, 2007

R. Montes December, 2016, Mechanical Rock Excavation ; *Theoretical And Experimental Results From Laboratory Tests Through An ILCM, Politecnico di Torino, Italy*

Rick P Lovat and P Eng. Tbm design considerations: selection of earthpressure balance or slurry pressure balance tunnel boring machines. InInt.Symp. on Utilization of underground space in urban areas, pages 6–7, 2006.

Rispoli, A., 2013. Analisi teorico-sperimentale per l'ottimizzazione dello scavo meccanizzato con utensili a disco, Torino: s.n.

Saffet Yagiz, Candan Gokceoglu, E Sezer, and Serdar Iplikci. Applica-tion of two non-linear prediction tools to the estimation of tunnel boringmachine performance.Engineering Applications of Artificial Intelligence,22(4-5):808–814, 2009

Shizhu Wen and Ping Huang. Tribology principle, 2002.

SR Torabi, H Shirazi, H Hajali, and M Monjezi. Study of the influence of geotechnical parameters on the tbm performance in tehran–shomal highwayproject using ann and spss.Arabian Journal of Geosciences, 6(4):1215–1227, 2013

Thomas R Kuesel, Elwyn H King, and John O Bickel.Tunnel engineeringhandbook. Springer Science & Business Media, 2012

URL -1 ; Kenneth S. Lane, Encyclopedia Britannica, Tunnel And Underground Excavation, "https://www.britannica.com/technology/tunnel" cited 10/03/2020.

URL-2 ;Wiley Book, "https://application.wiley-vch.de/books/sample/3433016763_c01.pdf" cited 10/03/2020

URL-3 ; Wikipedia,"https://commons.wikimedia.org/wiki/File:Beaumont tunnelbohrmaschine.png" cited 15/03/2020.

Vittorio Guglielmetti, Piergiorgio Grasso, Ashraf Mahtab, and Shulin Xu.Mechanized tunnelling in urban areas: design methodology and constructioncontrol. CRC Press, 2008

Yucong Pan, Quansheng Liu, Jianping Liu, Xing Huang, Qi Liu, andXingxin Peng. Comparison between experimental and semi-theoretical disccutter cutting forces: implications for frame stiffness of the linear cuttingmachine.Arabian Journal of Geosciences, 11(11):266, 2018

Yucong Pan, Quansheng Liu, Jianping Liu, Qi Liu, and Xiaoxuan Kong.Full-scale linear cutting tests in chongqing sandstone to study the influenceof confining stress on rock cutting efficiency by tbm disc cutter.Tunnelling and Underground Space Technology, 80:197–210, 2018